CALIFORNIA STATE UNIVERSITY, NORTHRIDGE

Combating an Intrinsic Antibiotic Resistance Mechanism by Interfering with Small RNA Regulation of an Outer Membrane Porin

A thesis submitted in partial fulfillment of the requirements

For the degree of Master of Science in Biology

By

Arada John Batresian

August 2021

The thesis of Arada Batresian is approved:

David Bermudes, Ph.D.	Date
Cristian Ruiz Rueda, Ph.D.	Date
Melissa Takahashi, Ph.D. – Chair	Date

California State University, Northridge

ACKNOWLEDGEMENTS

This project was only possible through the incredible support, knowledge, and help of many people. My thesis advisor, Dr. Melissa Takahashi, guided me through the many challenges of graduate school, celebrated my successes, and pushed me to become a better scientist and person. Thank you for the opportunity to work in your lab! I want to thank my committee members Dr. David Bermudes and Dr. Cristian Ruiz Rueda for their incredible wealth of knowledge on my subject matter, and for forcing me to chase my curiosity in my science journey. Finally, I could not do this without my lab mates and especially our lab technician Aaron Stibelman who supported me in every step of the way, and always made me laugh.

I am also forever grateful for the incredible support of my friends and family through my academic endeavors. Thank you for keeping me sane during a world pandemic; I am so grateful for our amazing little cohort, the grad students before me who taught me how to thrive in CSUN, and the amazing current grad students who have become lifelong friends. Much love to my family who supported me from 8,000 miles away; biggest thanks to my wife Melanis who took a leap of faith and supported me throughout my master's journey. Life without you would be meaningless.

TABLE OF CONTENTS

LIST OF TABLES

LIST OF FIGURES

ABSTRACT

Combating an Intrinsic Antibiotic Resistance Mechanism by Interfering with Small RNA Regulation of an Outer Membrane Porin

By

Arada John Batresian

Master of Science in Biology

The discovery of novel antibiotics has not kept pace with the growing threat of bacterial resistance. Bacteria have remarkable genetic plasticity that allows them to respond to a wide array of environmental threats, including the presence of antibiotic molecules that may jeopardize their existence. Compared to Gram-positive species, Gram-negative bacteria are intrinsically resistant to many antibiotics due to the presence of an outer membrane. Permeability through the outer membrane is the first step involved in the resistance of bacteria to an antibiotic. Among several outer membrane porins, outer membrane porin F (OmpF), is one of the largest porin proteins that enable the entry of several antibiotics. Therefore, the loss of OmpF highlights a devastating effect on the success rate of the current antimicrobial agents. The MicF sRNA is a small, antisense RNA found in *Escherichia coli* and related bacteria that shows extensive sequence complementarity with the 5' end of *ompF* mRNA and negatively regulates expression of OmpF, by hybridizing to *ompF* at its ribosome-binding domain and start codon. In this case, peptides engineered to bind to MicF specifically would interfere with its capacity to bind to *ompF*. ARMs are an excellent candidate for the design and selection of the peptides since they

are known to bind RNA effectively and specifically, as well as having cell penetrating abilities. By using the arginine-rich RNA-binding motifs (ARMs) as a framework, a random mutation peptide library was developed to produce peptides that have enhanced binding affinity for the MicF sRNA. Bacterial fluorescent colony selection was established as a rapid screening method to identify specific peptides available from a library containing thousands of peptide molecules using a fluorescent reporter. Two peptides with a high binding affinity for MicF were successfully discovered and the altered areas of these peptides were thoroughly investigated. Furthermore, the efficiency of these peptides in countering the effects of MicF mediated antibiotic resistance was demonstrated by minimum inhibitory concentration analysis. The *E. coli* MG1655 bacteria appear to be 30 percent more susceptible to antibiotics tested on average when the developed peptides were present inside the cell. In conclusion, this study focuses on the design and screening of the peptide molecules capable of binding to sRNA targets and aims to pave the way for future discussions about how targeting sRNAs could aid in the fight against drug-resistant infections.

CHAPTER 1: INTRODUCTION

Antibiotics revolutionized the treatment of infectious diseases in the 20th century and are some of the most powerful agents for fighting life-threatening infections [1][2]. Unfortunately, bacteria have developed mechanisms to resist the effect of the drugs that were developed to combat them. In fact, antibiotic-resistant bacteria represent one of the greatest global public health challenges of modern medicine [3]. As the number of resistant bacteria grows over time, even common infections, such as urinary tract infections, become more difficult to treat and can become life-threatening [4]. In 2019 the Centers for Disease Control and Prevention (CDC) indicated that antibiotic-resistant bacteria account for more than 2.8 million infections and cause 35,000 deaths, annually in the United States [3]. Furthermore, the direct cost of treatment in 2019 for antibiotic-resistant infections in the U.S. was approximately $20 billion, with an additional cost to society for lost productivity as high as $35 billion a year. It is projected that in the next 30 years, antibiotic-resistant infections are going to overtake cancer as the leading cause of death around the world, and based on current population estimates, resistant strains of bacteria could kill one person every three seconds [5].

At the beginning of the twentieth century, illnesses caused by microorganisms and particularly bacteria ranked among the most common causes of death worldwide [6]. By the middle of the century, dramatic advances in the prevention, management, and diagnosis of infectious diseases had occurred, and hopes were raised that many infectious diseases would be eliminated by the end of the 20th century. Much of this success in the management of infectious diseases was related to a continuous new armamentarium of antibiotics. The discovery of

penicillin by Fleming in 1928 followed by the discovery and clinical use of sulfonamides in the 1930s heralded the age of modern medicine [7]. Penicillin came into widespread use during the early 1940s [8]. By the 1950s, the 'golden era' of antibiotic development and use was well underway, and multiple new classes of antibiotics were introduced over the next two decades. These new antibiotics garnered such enthusiasm during the late 1960s and 1970s that some experts believed that infectious diseases would be conquered [9]. Unfortunately, since then resistance to nearly all antibiotics has been observed and despite this increase in antimicrobial resistance, the development of new antimicrobial agents is declining [10]. The ways we have developed and used antibiotics have led, predictably, to our current crisis of rising antibiotic resistance and declining new treatments. If we want to stave off a post-antibiotic era, we need to fundamentally change our approach. The fight against antibiotic-resistant bacteria using novel classes of antimicrobial agents has been played over so many times that we tend to find the same molecules over and over again [11]. Thus, moving forward the discovery of novel strategies that advance our ability to disrupt the expression of traits that protect bacteria against current antibiotics, and in turn increase, the efficacy of antibiotic therapy, are necessary [12].

Bacteria have remarkable genetic plasticity that allows them to respond to a wide array of environmental threats, including the presence of antibiotic molecules that may jeopardize their existence. They may manifest resistance to antibacterial drugs through a variety of mechanisms, in which several mechanisms of antimicrobial resistance are readily spread to a variety of bacterial genera through horizontal gene transfer. There are three major categories of antibiotic resistance mechanisms: (1) modification or degradation of the antibiotic; (2) modification of the antibiotic target; and (3) reduction of intracellular antibiotic concentration [13]. In order to reduce intracellular antibiotic concentrations, bacteria have developed mechanisms to regulate

both influx and efflux of antibiotics. The former mechanism prevents the antibiotic from reaching the intracellular or periplasmic target by limiting the uptake of the antimicrobial molecules [14]. Should an antibiotic find its way inside the cell; the latter mechanism clears out any toxic compounds by using efflux pumps. As the name implies, these pumps are multidrug transporters that are capable of pumping out a wide range of unrelated antibiotics, thus significantly contributing to multidrug-resistant organisms [15]. Many of the antibiotics used in clinical practice have intracellular bacterial targets therefore, these mechanisms significantly reduce the antimicrobial effect of existing antibiotics. In fact, the delivery of antibiotics inside cells is one of the major challenges of modern pharmaceutical research studies [13].

Compared to Gram-positive species, Gram-negative bacteria are intrinsically less permeable to many antibiotics as their outer membrane serves as a permeability barrier. The control of bacterial membrane permeability is a complex process that is tightly regulated by an intricate network of systems that sense and respond to osmotic shock, pH, temperature, antibiotics, and chemical stress [16]. Most hydrophilic and amphiphilic antibiotics cross the outer membrane by diffusing through outer membrane porin proteins [17]. Besides their role as hydrophilic channels, porins contribute to membrane stability and participate in various physiological processes [18]. There are two main ways in which bacteria can limit the uptake of antimicrobial agents through porins: (1) by decreasing the number of porins present in the outer membrane, and (2) mutations that change the selectivity of the porin channels [19]. Among several outer membrane porins, outer membrane porin F (OmpF), is an important transmembrane pore that facilitates the passages of hydrophilic solutes up to an exclusion size of approximately 600 kilodaltons, which enables entry of several antibiotics [20]. Several classes of antibiotic, such as β-lactams or fluoroquinolones, pass through the outer membrane via OmpF [21]. In

many in vivo studies, mutations to OmpF residues have been proven to substantially decrease susceptibility to antibiotics [22][23][24]. Additionally, mutants identified to be resistant to different families of antibiotics have been proven to lack the OmpF pore protein. Therefore, the loss of OmpF highlights a devastating effect on the success rate of the current antimicrobial agents [25].

The number of OmpF porins in the outer membrane of a bacterial cell affects its ability to allow nutrient uptake as well as its susceptibility to toxic compounds. The expression of *ompF* is regulated at the transcriptional and post-transcriptional levels. When the environment surrounding the bacteria has low osmolarity, a single *Escherichia coli* cell has been estimated to possess up to 10^6 OmpF proteins, [26] which facilitates the influx of nutrients. In contrast, in nutrient-rich environments where the osmolarity is high, it is detrimental for the cell to express a high level of OmpF. Therefore, under high-osmolarity conditions, there is a downregulation of OmpF, leading to the limited influx of nutrients, as well as toxic chemicals and antibiotics. This response is mediated by the two-component regulatory proteins OmpR-EnvZ at the transcriptional level [27]. Under high osmolarity conditions, a transmembrane sensor EnvZ autophosphorylates and transfers the phosphate group to OmpR, which in turn downregulates the expression of OmpF due to the low-affinity binding site in the *ompF* promoter region. In addition to the two-component system, when *E. coli* encounters antibiotics, as well as other environmental signals, such as high temperature, oxidative stress, or salicylate, it modulates the expression of OmpF via the upregulation of the small RNA (sRNA) MicF, which inhibits OmpF translation [28]. MicF shows extensive sequence complementarity with the 5’ end of OmpF

mRNA and negatively regulates expression of OmpF, by hybridizing to OmpF mRNA at its ribosome-binding domain and start codon (Figure 1) [29].

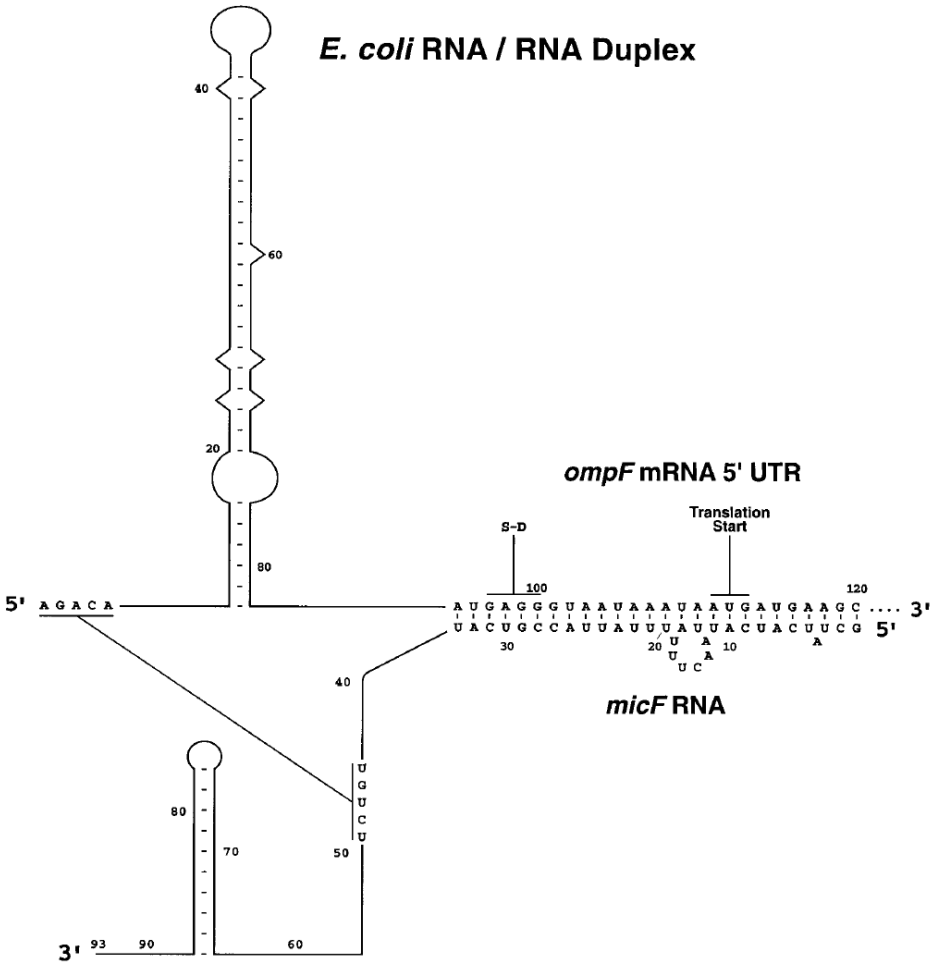

***Figure 1*. Predicted binding of MicF sRNA to ompF mRNA in *E. coli*.** The translation start site is indicated by AUG and the Shine-Dalgarno ribosome binding site as S-D. Adapted with permission from [30]

MarA, SoxS, and Rob are transcriptional regulators known to activate *micF* expression in response to environmental factors such as exposure to weak acids, oxidative stress, and cationic peptide antibiotics, respectively [31][32]. For example, antibiotics bind to the receptors inside the bacteria leading to activation of global regulatory genes which leads to the activation of transcriptional regulators that bind to the promoter region of MicF resulting in transcription of MicF. In an experiment, where the *micF* gene has been knocked out, *E. coli* showed increased

susceptibility to several antibiotics including norfloxacin and several cephalosporin antibiotics [33]. Although the OmpR-EnvZ transcriptional regulation of *ompF* does respond to the presence of antibiotics, post-transcriptional regulation by MicF provides a more rapid response to the environmental condition [34].

The increased expression of MicF modulates outer membrane permeability, [35] hence reducing the effectiveness of the current antibiotics [36]. One way to limit the emergence of this type of resistance and preserve the usefulness of currently available antibiotics would be to prohibit the repression of OmpF porin by preventing the hybridization of MicF and *ompF* mRNA [12]. **Here, I hypothesize that a designed molecule, capable of binding to MicF, would prevent MicF from binding to its ultimate target, *ompF* mRNA. This will create a domino effect ending with the normal number of OmpF on the cell surface, allowing the antibacterial agents to enter the cell and eventually manifesting their destructive effects on the cell.**

Antisense RNAs (asRNA) are an obvious candidate to prohibit the MicF and *ompF* mRNA hybridization. Antisense RNAs are small, noncoding, RNAs that complement mRNA [37]. Such molecules have the ability to bind to their targets through Watson-Crick base pairing, thus are easily designed. However, as simple as this concept sounds, clinical success has been out of reach. New medicinal chemistry is needed to make asRNAs more potent and less immunogenic, and the delivery hurdle – getting the drug into the target bacterial cell – has been a major setback [38]. An alternative candidate to prevent the repression of *ompF* through binding to MicF is peptide molecules. Peptides have been specifically more effective in reaching their ultimate target inside cells. The use of cell-penetrating peptides (CPPs), such as the minimal sequence of Penetratin (RRMKWKK), has facilitated the translocation across the cell membrane

and eased the delivery of peptides allowing them to carry out their biological function [39]. Furthermore, there are peptides that are known to bind RNAs with high affinity and specificity through a variety of RNA-binding domains and are involved in regulating the fate and function of the bound RNA [40]. The amino acid sequence of a peptide will define its function and specificity for the target RNA. For instance, a number of proteins containing arginine-rich motifs (ARMs) are known to bind RNA and are involved in regulating RNA processing in viruses and cells [41].

Arginine-rich RNA-binding domains are found in a relatively large group of proteins and specifically recognize their RNA targets even as short (<20 amino acid) isolated peptides [42]. ARMs appear to have arisen independently throughout phylogeny. For example, the ARM of the lambdoid bacteriophage N protein binds hairpin loops in nascent RNAs to regulate antitermination, [43] while the ARM of the Human Immunodeficiency Virus (HIV)-1 Rev protein binds to a 50 nucleotide region of the HIV genome, and regulates mRNA transport and splicing [44]. As shown in Figure 2, a comparison between the Bovine immunodeficiency virus (BIV) Tat peptide (17 amino acids) and the HIV Tat peptide (15 amino acids) with their corresponding TAR RNA complexes shows how two RNAs that are similar in structure can be recognized by arginine-rich peptides using entirely different peptide conformations and amino acid–RNA interactions for recognition [45].

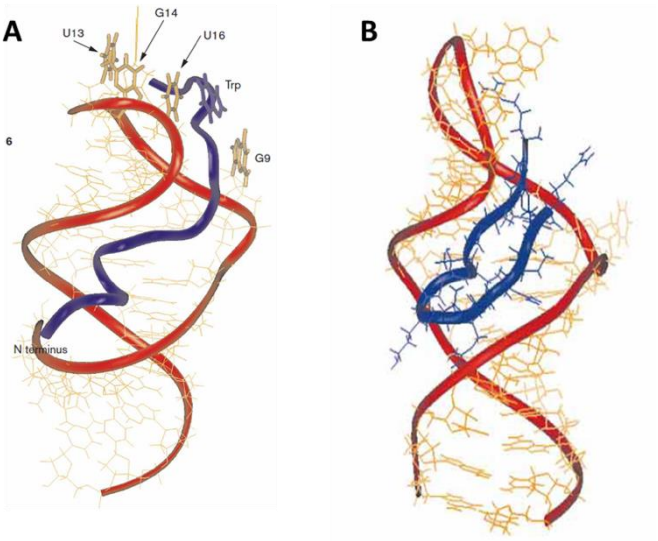

Figure 2. **NMR structures of peptide–RNA complexes.** A) NMR model of the HIV-1 Tat–TAR complex B) BIV Tat–TAR complexes. Peptides are in blue and RNAs in red and orange. Adapted with permission from[42].

ARMs have the potential to be a framework for the design and selection of RNA-binding molecules to bind MicF for several reasons: (1) there are multiple well-studied examples of ARMs that occur in nature that bind to RNA hairpin structures similar to the hairpin in MicF's secondary structure [46]; (2) the specificity of binding of ARMs can be altered by randomizing amino acids [47]; (3) there are known examples of tryptophan and arginine-rich antimicrobial peptides that are able to penetrate bacterial membranes [23]; and (4) upon initial binding of the ARMs with their cognate RNA, structural changes occur in the peptide to allow for more adaptive binding. **Therefore, the goal of this study is to design a peptide by randomizing regions of well-studied ARMs to change their specificity to bind to MicF; thus, disrupting its ability to bind to *ompF*.**

Out of many ARMs known to have RNA binding characteristics, four specific ones were chosen that showed a promising horizon in RNA regulation and can be altered to bind to MicF [42]. These include the N protein from the λ and P22 phages, the Tat protein of BIV, and the Rev protein of HIV-1. Previous studies had shown the effectiveness of the peptides mentioned above

in recognizing their specific target RNA as well as changing the fate of the bound RNA. For instance, a viral transcriptional activator, BIV Tat binds specifically to TAR mRNA and a single arginine provides the only sequence-specific contact [48]. There have been many studies exploring the binding structure of the HIV1 REV peptide and its cognate RNA REV responsive element (RRE). One study showed that a number of alanine substitutions in the arginine fork increases the affinity of REV protein for its cognate RNA [49].

Given the versatility of these arginine-rich motifs, and the ability to modify their interactions with RNAs, this study aims to discover peptides capable of binding MicF by randomizing the starting peptide sequence. This study paves the way for the development of novel sequence-specific proteins that bind to RNA targets. Here the development of bacterial fluorescent colony selection is introduced as a rapid screening method to identify specific peptides from a library containing thousands of peptide molecules using a fluorescent reporter. Bacterial fluorescent colony selection is then used to screen the randomization of the candidate peptides in the sections known to add specificity and binding affinity. Two peptides with the highest specificity for MicF are selected, the altered sections of these peptides are thoroughly investigated, and new designs are considered. Finally, the efficiency of the peptides in countering the effects of MicF on antibiotic-resistant mutations are further demonstrated by minimum inhibitory concentration analysis.

CHAPTER 2: MATERIAL AND METHODS

Bacterial strains and growth conditions:

E. coli strains were grown in LB (Lysogeny broth) medium or on LB plates containing 1.5% agar in the presence of appropriate antibiotics. Three antibiotics were used throughout the experiments with the following concentrations: carbenicillin (100 µg/ml), chloramphenicol (34 µg/ml), kanamycin (50 µg/ml). Plasmids were propagated in *E. coli* NEB Turbo cells (New England Biolabs) (F' proA + B + lacI q ΔlacZM15/fhuA2 Δ(lac-proAB) glnV galK16 galE15 R(zgb-210::Tn10) TetS endA1 thi-1 Δ(hsdS-mcrB)5) [50] and *E. coli* MG1655 (F- lambda- ilvG- rfb-50 rph-1) [51].

Chemically competent cells

Fresh colonies of *E. coli* NEB Turbo cells (New England Biolabs) or *E. coli* K12 MG1655 were isolated through plating on 1.5% LB agar. A single colony was inoculated into 5 ml of LB media overnight. The entire overnight culture was inoculated into 500 ml of pre-warmed LB media to allow growth to early log phase (OD600 reading of 0.3–0.5) followed by immediate placement on ice for 15 minutes and centrifugation at 3500 rpm for 10 minutes at 4°C. The supernatant was removed, and the pellets were resuspended in 10 mL of the ice-cold, sterile-filtered TSS buffer (LB broth with 10% (wt./vol) PEG 3350, 5% (vol/vol) DMSO, and 2% (wt./vol) $MgCl_2$, at a final pH of 6.5). Aliquots of 200 µL resuspended mixture were made and then cells were transferred to -80°C for storage. The competent cells carrying the pMKT172 and pMKT173 were made following the same general procedure. The plasmids pMKT172 and pMKT173 were transformed into *E. coli* NEB Turbo cells (New England Biolabs) and plated on 1.5% LB agar containing chloramphenicol and carbenicillin. A single colony was inoculated into 5 ml of LB media containing both antibiotics.

Plasmid construction:

A table of all the plasmids used in this study can be found in the appendix of this document (Table 3). Gibson assembly was used to construct pMKT172, pMKT173, and plasmids containing peptides with the inducible promoter P_{lux}. Vector and insert DNA were created using PCR with the primers and plasmids indicated in Table 4. A DpnI digest was performed on the unpurified PCR products to cut the plasmid DNA templates by adding 1 µl of DpnI (NEB R0176L) directly to the PCR reaction. The tubes were incubated at 37°C for 1 hour. The digested product was then run on a 1% agarose gel and the appropriate size DNA fragments were purified using the QIAquick Gel Extraction Kit (Qiagen 28706X4) according to the manufacturer's protocol. Approximately 100 ng of the vector was mixed with a 3x molar excess of the insert to a final volume of 5 µl and was added to 15 µL of 1.33x Assembly Master mix for the Gibson assembly. The assembly master mix consisted of 5x Isothermal Reaction Buffer (25% PEG-8000, 500 mM Tris-HCl, 50 mM $MgCl_2$, 50 mM DTT, 1 mM dNTPs, 5 mM NAD, pH 7.5), T5 exonuclease (10U/µl), Phusion DNA polymerase (2U/µl), and Taq DNA ligase (40U/µl). The mixture was incubated at 50°C for 1 hour. The final Gibson assembly reaction was transformed into NEB turbo competent cells. To start the transformation, 30 µL of 5X KCM (0.5M KCl, 0.15M $CaCl_2$, 0.25M $MgCl_2$) was added to 200 µl of thawed competent cells and then 30 µl of the mixture was added to the Gibson assembly reaction and incubated on ice for 20 minutes. After heat shock at 42°C for 90 sec, 30µl of 2YT medium was added to the mixture. After 30 min recovering/ shaking at 37°C at 200 rpm, 6µl was plated onto the LB agar plate containing carbenicillin (100 µg/ml), chloramphenicol (34 µg/ml), or kanamycin (50 µg/ml) respectively. The plates were then incubated at 37°C overnight. Colonies from each construct were picked for inoculation in LB medium (with carbenicillin, chloramphenicol, or kanamycin

for each plasmid) and grown for 17 hours overnight at 37°C while shaking (200 rpm). Plasmid DNA was purified, and plasmids were sequence confirmed according to the protocol described in Plasmid purification and DNA Sequencing below.

Sequences for arginine-rich peptides were obtained from literature, codon-optimized for *E. coli*, and inserted into a ColE1 backbone with kanamycin resistance using inverse-PCR (iPCR). iPCR was also used to construct pMKT179, pMKT180, pMKT182, and pMKT184. Linear DNA was created using PCR with the primers and plasmids indicated in Table 3. Prior to PCR, primers were phosphorylated by adding 0.5 µl T4 Polynucleotide Kinase (10 U/µL) (ThermoFisher EK0032) to 10µl reaction containing 1µl of 100µM primer, 1µl T4 ligase buffer, and 7.5 µl nuclease-free water, and the tubes were incubated at 37°C for 1 hour. Following PCR, a DpnI digest was performed on the unpurified PCR products to cut the plasmid DNA templates by adding 1 µl of DpnI (NEB R0176L) directly to the PCR reaction. The tubes were incubated at 37°C for 1 hour. The digested product was then run on a 1% agarose gel and the appropriate size DNA fragments were purified using the QIAquick Gel Extraction Kit (Qiagen 28706X4) according to the manufacturer's protocol. Approximately 100 ng of the purified DNA was diluted to a final volume of 8.5 µl and was added to 1 µl 10x T4 ligase buffer to complete the ligation using 0.5 µL T4 DNA ligase (NEB M0202L). The mixture was incubated at 37°C for 30 minutes. The final ligation mixture was transformed into NEB turbo competent cells as described above for the Gibson assembly products.

Plasmids containing randomized peptides were constructed using iPCR following the same methods as above using NNN in specific locations of the peptide (see Table 5 for oligonucleotide sequences used). Upon completion of the ligation reaction, plasmids were transformed into the chemical competent cells carrying pMKT172 and pMKT173 following the

steps above. The entire transformation mixture was plated onto the LB agar plates containing carbenicillin and chloramphenicol and kanamycin (3 µl per plate). The plates were then incubated at 37°C overnight, placed at 4°C for 24 hours.

Bacterial fluorescent colony selection

Plates containing randomized peptides were stored at 4°C for 24 hours and then visually screened using a dark reader (Labgene Scientific DR46B) for green fluorescence. Selected colonies were then inoculated into the 300 µL of LB medium containing the three antibiotics in a 96-deep-well block (Costar 09-761-116A) for further analysis. The cultures were incubated for 17 hours overnight at 37°C while shaking at 200 rpm on a Labnet Vortemp benchtop shaker. Overnight cultures were diluted to an OD600 of 0.015 in 300 µl of fresh LB medium and grown for three hours. One hundred µl of each culture was transferred to 96 well plate (Corning 07-000-134) and fluorescence (excitation 485 nm, emission 520 nm) and OD600 (absorbance 600 nm) was measured using the Biotek Synergy H1 Hybrid Multi-mode reader.

Bacterial fluorescent colony selection data analysis:

Bulk fluorescence endpoint and Absorbance Endpoint were measured separately for each colony. Media blank average was measured and subtracted from each cell. The FL/OD was calculated for each well containing an individual colony. FL/OD for all colonies was then normalized over the antiMicF ctrl (pMKT174).

Plasmid purification and DNA Sequencing

Selected colonies from the previous steps were picked for inoculation in LB medium with appropriate antibiotics and grown for 17 hours overnight at 37°C while shaking (200 rpm). Plasmid DNA miniprep was performed using QIAprep Spin Miniprep Kit (QIAGEN, Valencia, CA, USA) according to the manufacturer's protocol. All the cloned sequences were finally

confirmed by DNA sequencing at the Laragen Inc (www.laragen.com), using primers mentioned in Table 3.

Bulk fluorescence experiment

Plasmids containing selected randomized peptides were constructed using iPCR following the same methods as above. Purified plasmids were transformed into the chemical competent MG1655 cells along with pMKT172 and pMKT173 following the steps above for the experiment. Cells with ompF-GFP (pMKT172) and control plasmids for p15A and ColE1 was used as the OmpF ON control. The OmpF OFF control was cells with ompF-GFP (pMKT172) and MicF (pMKT173), as well as control plasmid for ColE1. Moreover, ompF-GFP, MicF, and antiMicF1-33 (pMKT174) were used to create AntiMicF ctrl. For this purpose, only ompF-GFP (pMKT172) and the peptide, together with the p15A control plasmid were transformed into the *E. coli* MG1655. The control plasmids had the same promoter, terminator, backbone, resistance, and replication origin as the study plasmid, but it lacked the gene of interest. The entire transformation mixtures were plated onto the LB agar plates containing carbenicillin and chloramphenicol and kanamycin (3 µl per plate). The plates were then incubated at 37°C overnight.

Three colonies from each condition were then inoculated into the 300 µL of LB medium containing the three antibiotics in a 96-deep-well block (Costar 09-761-116A). The cultures were incubated for 17 hours overnight at 37°C while shaking at 200 rpm on a Labnet Vortemp benchtop shaker. Overnight cultures were diluted to an OD600 of 0.015 in 300 µl of fresh M9 minimal medium and grown for three and half hours. Fifty µl of each culture was transferred to 96 well plate (Corning 07-000-134) along with fifty µl of sterile water and fluorescence

(excitation 485 nm, emission 520 nm) and OD600 (absorbance 600 nm) was measured using the Biotek Synergy H1 Hybrid Multi-mode reader.

Bulk fluorescence data analysis:

Media blank average was measured and subtracted from each cell. The FL/OD was calculated for each well containing an individual colony. FL/OD for all replicates were then normalized over the OmpF ON signal since that is the ultimate fluorescence production. OmpF ON was measured from only the ompF-GFP with control plasmids replacing the MicF and the peptide in the chemical competent cells.

Minimum inhibitory concentration analysis (MIC):

Minimum inhibitory concentration analysis was performed for both of the candidate peptides (G28 and GH3) along with controls against two antibiotics: Norfloxacin and cephalothin. Plasmids containing G28, GH3 or control plasmid with inducible promoter (P_{lux}) were transformed into the chemical competent MG1655 cells following the steps described above. The entire transformation mixture was plated onto the LB agar plates containing kanamycin (3 µl per plate). The plates were then incubated at 37°C overnight. Upon successful growth, a single colony was inoculated into 5mL MOPS medium with added kanamycin and was grown for exactly 17 hours overnight.

On the third day of the analysis, antibiotic stocks of Norfloxacin (400µg/ml) and cephalothin (51,200µg/ml) and acyl-homoserine lactone (AHL) dilutions were prepared to start the fresh culture. 1mL of cells from the overnight culture was transferred into 1.7mL centrifuge tube and spun at 13,000 rpm for 1 minute. The overnight media was removed and replaced with fresh MOPS with no antibiotics. To create the master mix of the cells and the AHL, 5×10^5

CFU/mL of the cells in final culture was calculated and the final concentration of 10nM AHL was set to be added to the culture. Two hundred µl of master mix was distributed into columns 1-11 of a 96 well block. For the first column, extra 196 µl of master mix was added to increase the total volume of the well to 396µl. Four µl of appropriate antibiotic was added to column 1 and mixed by pipetting. The stock concentrations mentioned above were calculated precisely and made fresh every day. Two-fold serial dilutions were performed from column 1 to column 10 by transferring two hundred µl of master mix with antibiotic to the adjacent well. Two hundred µl was discarded from all wells of column 10 to have an equal volume of 200 µl in each well. Two hundred µl of freshly made MOPS media was added to the column 12 with no cells or antibiotics to generate the media blank. The 96 well block was then sealed with breathe easy film (Diversifie Biotech Cat. No.: BEM-1) and shaken/incubated at 1000rpm at 37C for 24 hours.

On day 4 of the analysis, one hundred µl of the overnight culture was transferred onto 96 well plate and OD600 (absorbance 600 nm) was measured using the Biotek Synergy H1 Hybrid Multi-mode reader.

CHAPTER 3: RESULTS

Bacterial fluorescent colony selection

This study is set to identify the most specific and effective peptide that binds to MicF and sequesters MicF from binding to *ompF* mRNA. To start, it was necessary to develop a method to quickly screen thousands of peptide candidates and identify those that interfere with MicF regulation. Bacterial fluorescent colony selection through the simultaneous transformation of three plasmids was determined to be an ideal method to continue (Figure 3A). This was achieved by fusion of the 5' UTR region of the *ompF* to the green fluorescent protein (GFP) as a reporter to monitor the effective prevention of the MicF binding due to candidates from a library of peptides. Three plasmids were constructed to carry ompF-GFP, MicF, and the candidate peptides separately. This approach would create a concentration gradient with the peptide being the highest, followed by MicF, and ompF-GFP on the lowest copy plasmid. After the simultaneous transformation of all three plasmids, each peptide candidate is carefully screened for effective binding to MicF. Colonies containing effective peptides would turn green because if the candidate peptide was effective in binding to MicF, it would sequester it from reaching ompF-GFP. On the other hand, if the peptides were ineffective in binding to MicF, then MicF would bind to the RBS site of the *ompF* 5' UTR and would repress the translation of GFP resulting in white colonies. Initial screening of colonies is done visually by the naked eye and also on a dark reader. Afterward, selected green colonies are grown in LB media with appropriate antibiotics and bulk fluorescence endpoint, and absorbance is measured separately for each colony to confirm GFP expression. AntiMicF 1-33, created by Takahashi lab, was utilized to test the screening procedure with a proper control. AntiMicF 1-33 is an antisense molecule that has been developed particularly to bind to MicF. In cell-free reactions, where biological gene expression is

harnessed inside non-living, in vitro biochemical reactions, this molecule has been shown to be an effective agent for binding to MicF, hence recovering the fluorescence signal (Figure 4A). To begin developing the screening method, ompF-GFP, MicF and antimicF 1-33 were all transcribed from the J23119 constitutive promoter, which is the strongest promoter from the Anderson promoter library [52]. While the use of J23119 was great for visual confirmation of GFP, even without the dark reader, this placed a high burden on the cells. Transformed colonies grew very slowly and often would not transform at all. Several other members of the Anderson promoter collection were tested for effective cell growth and gene expression and J23118 was selected for the screening platform. Unfortunately, the green colonies were not identifiable by the naked eye, however, the colonies were easily distinguishable when set on the dark reader.

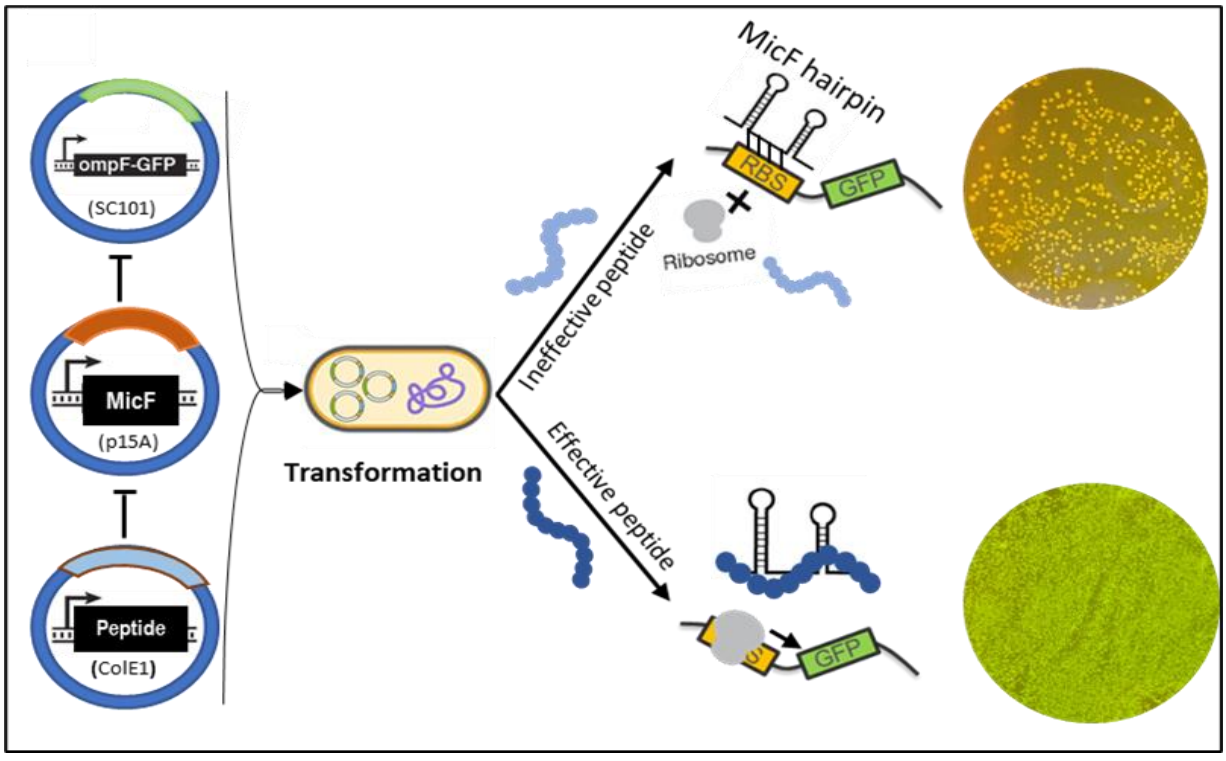

***Figure 3*. Schematic representation of experimental setup.** By randomizing the amino acids known to be involved with RNA binding, libraries of peptide sequences will be created. Plasmids containing the peptide library will be transformed into *E. coli* along with two other plasmids each containing the ompF-GFP reporter and the MicF, respectively. In presence of an effective peptide, the binding of the MicF to ompF will be interrupted and therefore GFP production will be increased upon growth in the presence of antibiotics. (chloramphenicol, carbenicillin, kanamycin), colonies will be visually screened and those with the highest GFP fluorescence will be chosen.

The recovery of the fluorescence signal, using the antimicF 1-33, in the same manner as the cell-free reactions was a hurdle in verifying the bacterial fluorescent colony selection. Cell-free reactions demonstrated its effectiveness to recover the fluorescence signal one hundred percent (Figure 4A). When the molecule was tested in vivo using the J23118 promoter from Anderson's library, it only recovered roughly fifty percent of the signal (Figure 4B). Among numerous explanations for the difference in fluorescence recovery rates, the concentration ratio between cell-free reactions and the bacterial fluorescence colony section stood out. This is owing to the fact that cell-free reactions allow for complete control of molecular concentrations. In the three-plasmid system, however, all of the genes were expressed with the same J23118 constitutive promoter, leaving the concentration ratios to be determined only by the plasmid copy number. To investigate if concentration was the key to recovering the fluorescence signal at a higher rate than the J23118 promoter, the P_{lux} inducible promoter was used to synthesize antiMicF 1-33 in *E. coli*. P_{lux} upregulates the expression of downstream genes when the LuxR activator protein is complexed with the inducer 3-oxo-C6-HSL (AHL), allowing overexpression of a gene without placing the cells under too much stress during transformation. At 10nM AHL the fluorescence signal was restored to one hundred percent (Figure 4C). While using the P_{lux} promoter restores the fluorescence signal to 100%, it necessitates picking and inducing the colonies in the culture with the 10nM AHL concentration. J23118, which does not require induction but still turns the cells green on the plate and allows colonies to be selected based on green fluorescence production, was used for screening the randomized peptides, and AntiMicF

ctrl was added for comparing the randomized peptides to the antiMicF throughout the experiments.

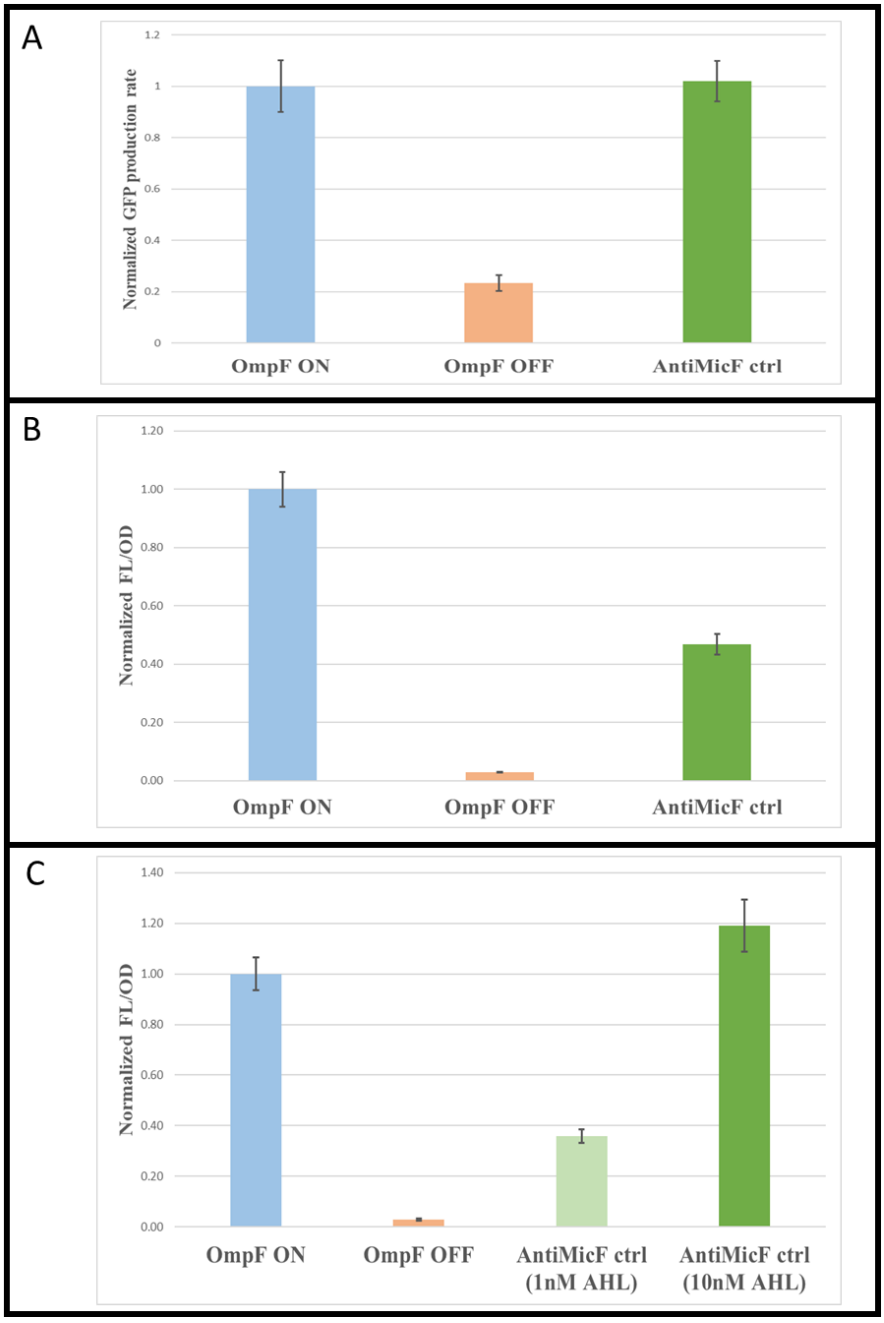

Figure 4. **In vivo troubleshooting of the AntiMicF ctrl for validation of bacterial fluorescent colony selection.** (A) Performance of antimicF 1-33 in cell-free reactions. Production of the GFP is normalized to the ompF ON condition. (B) In vivo measurements of antimicF fluorescence signal with J23118 constitutive promoter normalized over ompF ON. (C) In vivo measurements of antimicF fluorescence signal with P_{lux} inducible promoter with different AHL concentrations normalized over ompF ON. All the error bars are representing standard deviations from three replicates.

After the successful development of the screening method, all four natural peptides, N protein from the λ and P22 phages, the Tat protein of BIV, and the Rev protein of HIV-1, were tested against MicF to explore if they show any natural binding to MicF.

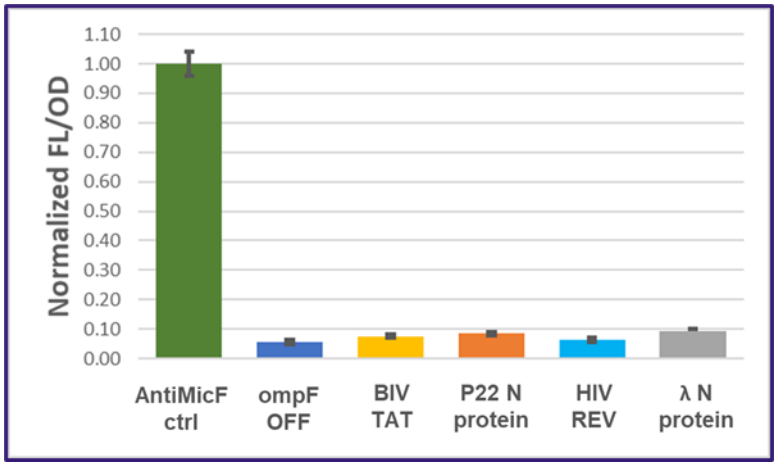

Figure 5. **Fluorescence measurements to investigate if natural ARMs sequester MicF from binding to ompF.** AntiMicF ctrl only carries ompF-GFP, along with AntiMicF 1-33 without MicF and demonstrates the highest GFP translation recovery possible in the experiment. Error bars represent the standard deviation from three biological replicates.

As shown in Figure 5, none of the four natural peptides showed a substantial increase in the development of GFP. As a result, the first round of randomization was performed on all four peptides.

Randomization of Bovine Immunodeficiency Virus (BIV) Tat protein

There are two regions within BIV Tat known to be important for binding affinity and specificity of the cognate RNA Figure 5A[53]. The first region, denoted as A, includes the amino acids in positions 4 (Gly) and 5 (Thr). The second region, denoted as B, includes the amino acid in position 7 (Gly). Candidate peptides were generated by randomizing regions A and B independently and collectively to identify the best approach. As seen in Figure 6, colonies from the BIV Tat randomization did not produce any significant improvement compared to the natural peptide.

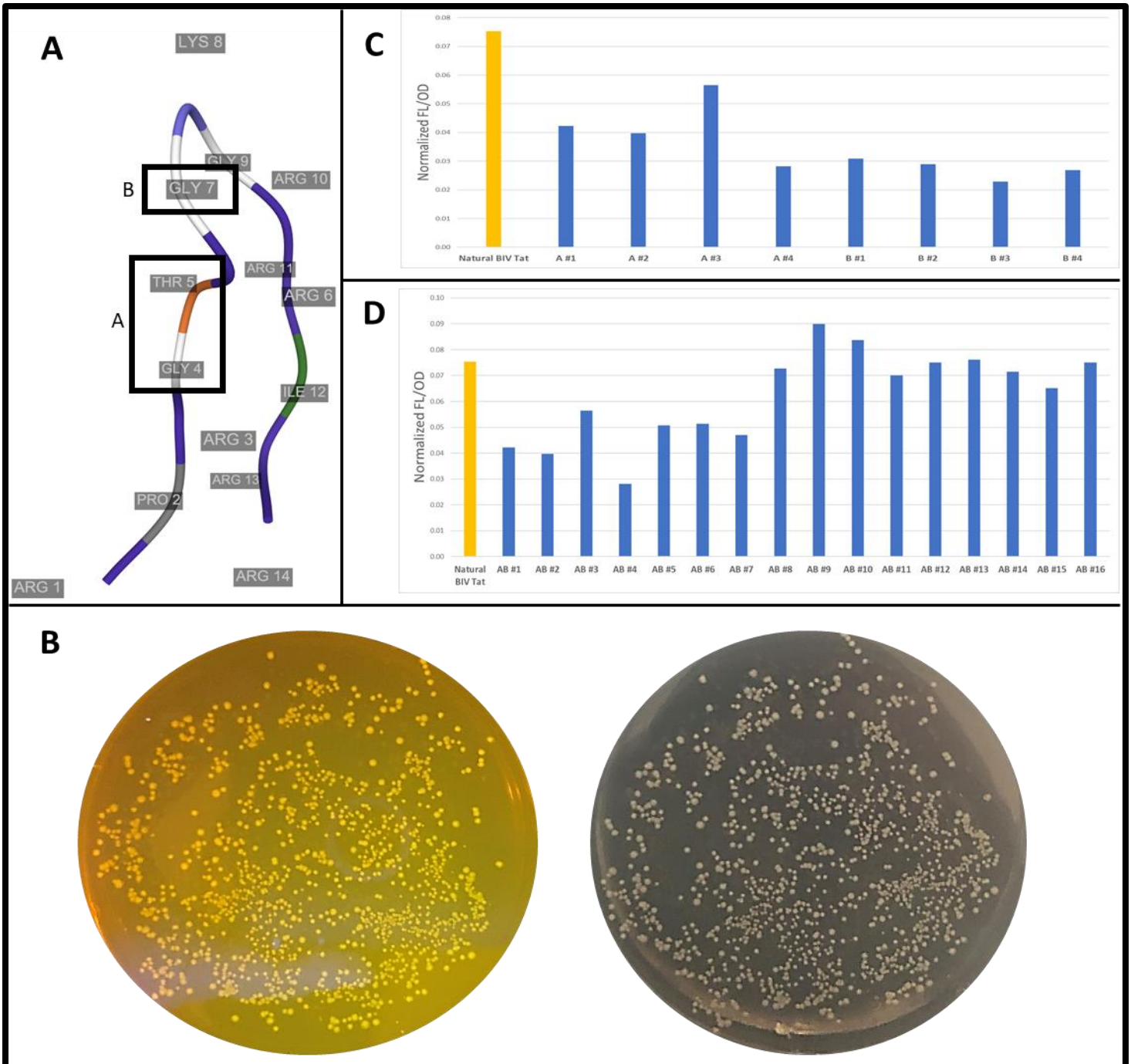

Figure 6. **Screening of randomized Bovine Immunodeficiency Virus(BIV) Tat protein** (A) Identification of amino acids on NMR model of BIV Tat peptide. Amino acids in position 4 (Gly) and 5 (Thr) were randomized together and called region A. The amino acid in position 7 (Gly) was randomized independently and called region B. (B) Representative plate from BIV Tat randomization. The image on the left represents the plate viewed on the dark reader and the image on the right is the plate viewed by the naked eye. (C) Fluorescence measurements of selected single region randomized colonies compared to the natural BIV Tat protein. (D) Fluorescence measurements of selected double region randomized (both regions A and B were randomized together) colonies compared to the natural BIV Tat protein. In (C) and (D) each bar represents one colony selected from the visual screening of the colonies. Each bar is normalized to the OmpF ON control.

Randomization of Bacteriophage P22 Probable regulatory protein N

There are two regions within the P22 phage N protein known to be important for binding affinity and specificity of the cognate RNA (Figure 7A)[54]. The first region, denoted as C, includes the amino acids in positions 1 (Asn), 2 (Ala), 3 (Lys), and 4(Thr). The second region, denoted as D, includes the amino acids in positions 12 (Lys), 13(Leu), 14(Ala), 15(Ile), and 16(Glu). Candidate peptides were generated by randomizing regions C and D independently and collectively to identify the best approach. As seen in Figure 7, colonies from the P22 N protein randomization did not produce any significant improvement compared to the natural peptide.

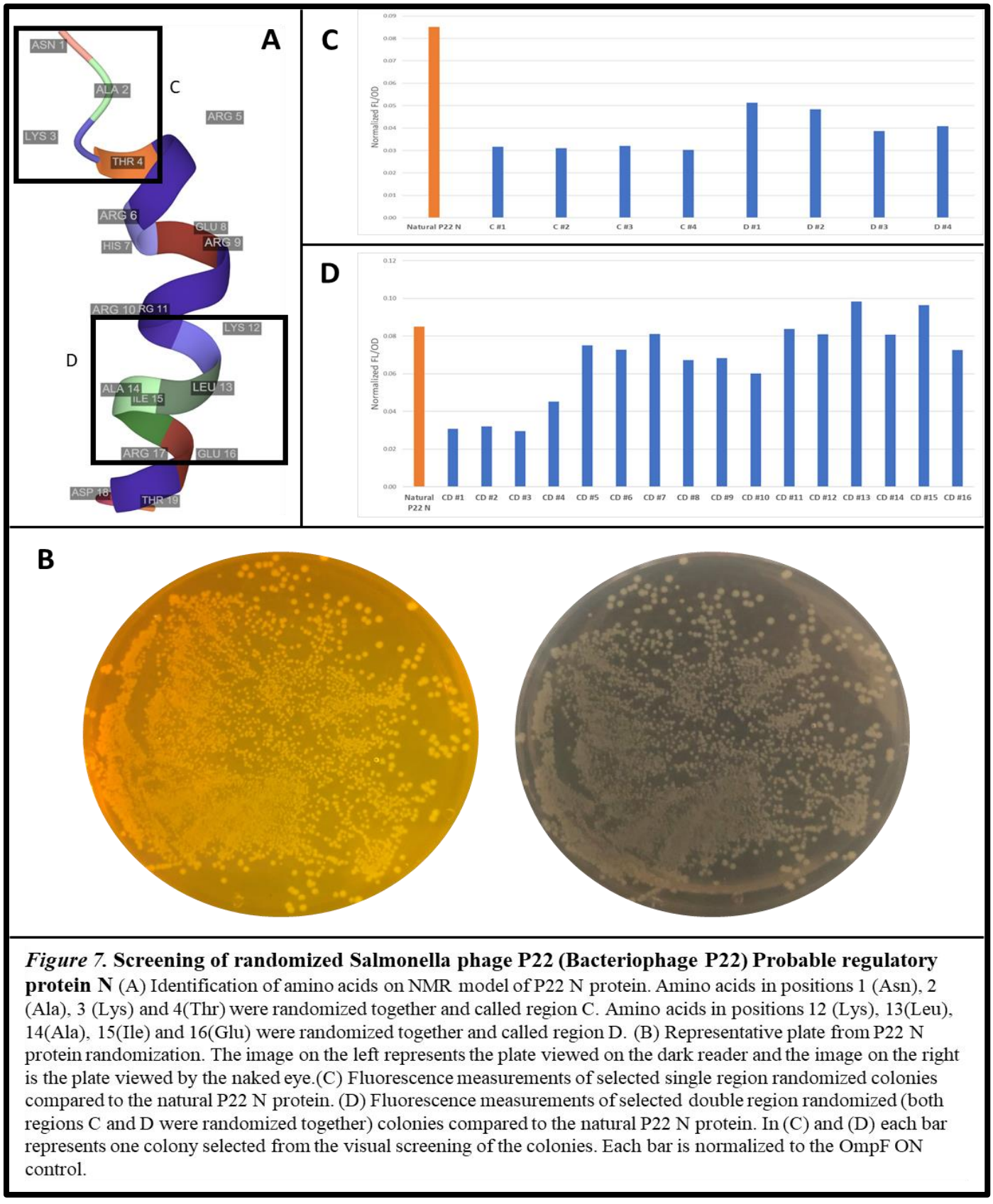

Figure 7. **Screening of randomized Salmonella phage P22 (Bacteriophage P22) Probable regulatory protein N** (A) Identification of amino acids on NMR model of P22 N protein. Amino acids in positions 1 (Asn), 2 (Ala), 3 (Lys) and 4(Thr) were randomized together and called region C. Amino acids in positions 12 (Lys), 13(Leu), 14(Ala), 15(Ile) and 16(Glu) were randomized together and called region D. (B) Representative plate from P22 N protein randomization. The image on the left represents the plate viewed on the dark reader and the image on the right is the plate viewed by the naked eye.(C) Fluorescence measurements of selected single region randomized colonies compared to the natural P22 N protein. (D) Fluorescence measurements of selected double region randomized (both regions C and D were randomized together) colonies compared to the natural P22 N protein. In (C) and (D) each bar represents one colony selected from the visual screening of the colonies. Each bar is normalized to the OmpF ON control.

Randomization of Human Immunodeficiency Virus Type 1 (HIV1) Protein REV

There is one region within the HIV1 REV protein known to be important for binding affinity and specificity of the cognate RNA (Figure 8A)[55]. The region, denoted as E, includes the amino acids in positions 2(Thr), 4(Gln), and 5(Ala). Candidate peptides were generated by randomizing regions E to identify the best approach. As seen in Figure 8, colonies from the HIV1 Rev protein randomization did not produce any significant improvement compared to the natural peptide.

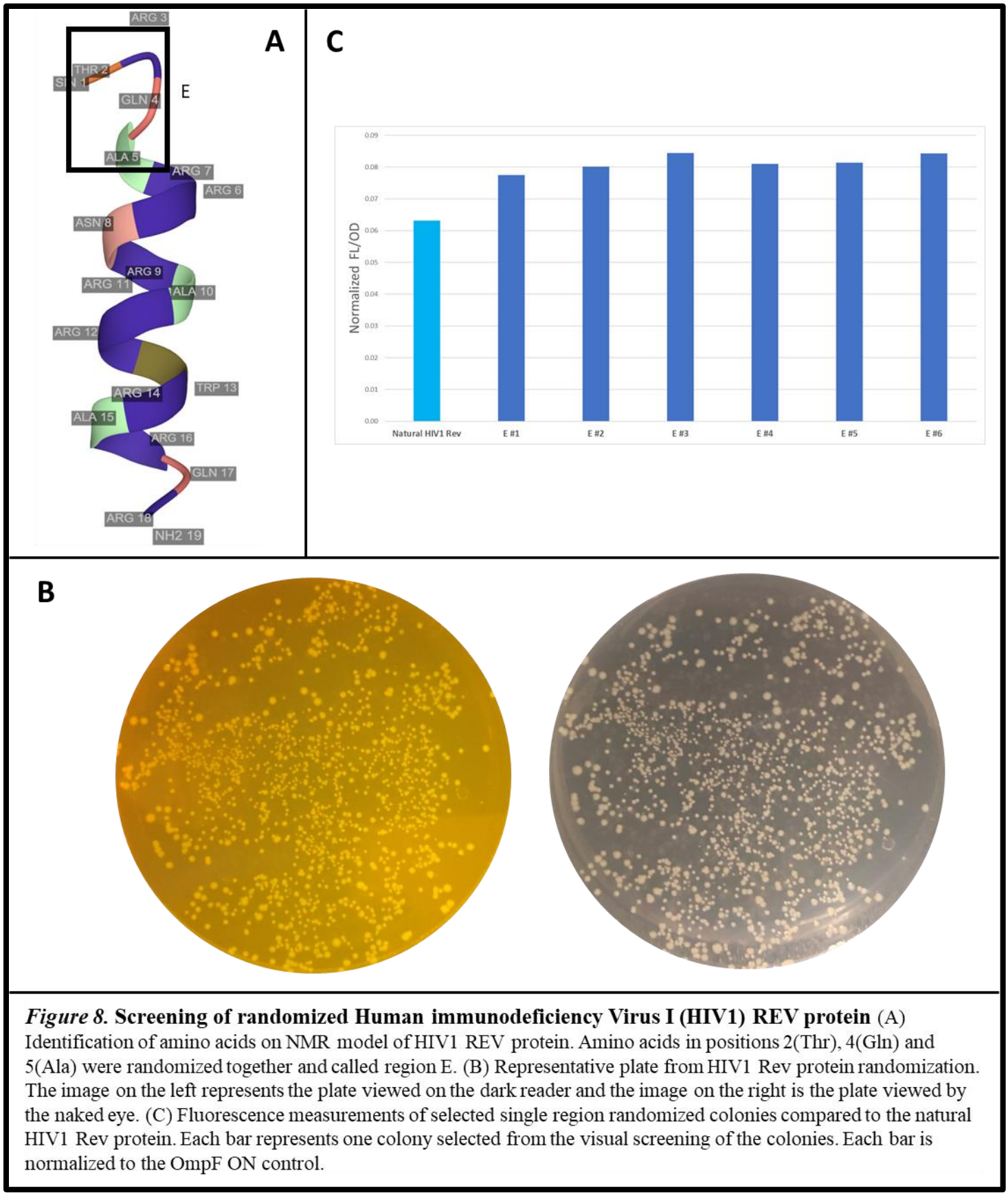

Figure 8. **Screening of randomized Human immunodeficiency Virus I (HIV1) REV protein** (A) Identification of amino acids on NMR model of HIV1 REV protein. Amino acids in positions 2(Thr), 4(Gln) and 5(Ala) were randomized together and called region E. (B) Representative plate from HIV1 Rev protein randomization. The image on the left represents the plate viewed on the dark reader and the image on the right is the plate viewed by the naked eye. (C) Fluorescence measurements of selected single region randomized colonies compared to the natural HIV1 Rev protein. Each bar represents one colony selected from the visual screening of the colonies. Each bar is normalized to the OmpF ON control.

Randomization of Bacteriophage lambda Antitermination N protein

N protein from bacteriophage λ appears to be a versatile peptide and has been widely used to target RNAs in previous experiments [56]. Initially two regions known to increase the specificity and affinity of binding between the peptide and the cognate RNA were identified as: amino acids in positions 2(Asp), 3(Ala), 4(Gln), and 5(Thr) (region G) and amino acids in positions 12 (Ala), 13(Glu), 14(Lys), and 15(Gln) (region F) Figure 9A. Again, candidate peptides were generated by randomizing regions F and G separately and collectively. As shown in Figure 9, in the first rounds of randomization, 12 peptides, represented in purple bars, demonstrated an increase in GFP fluorescence over the natural peptide.

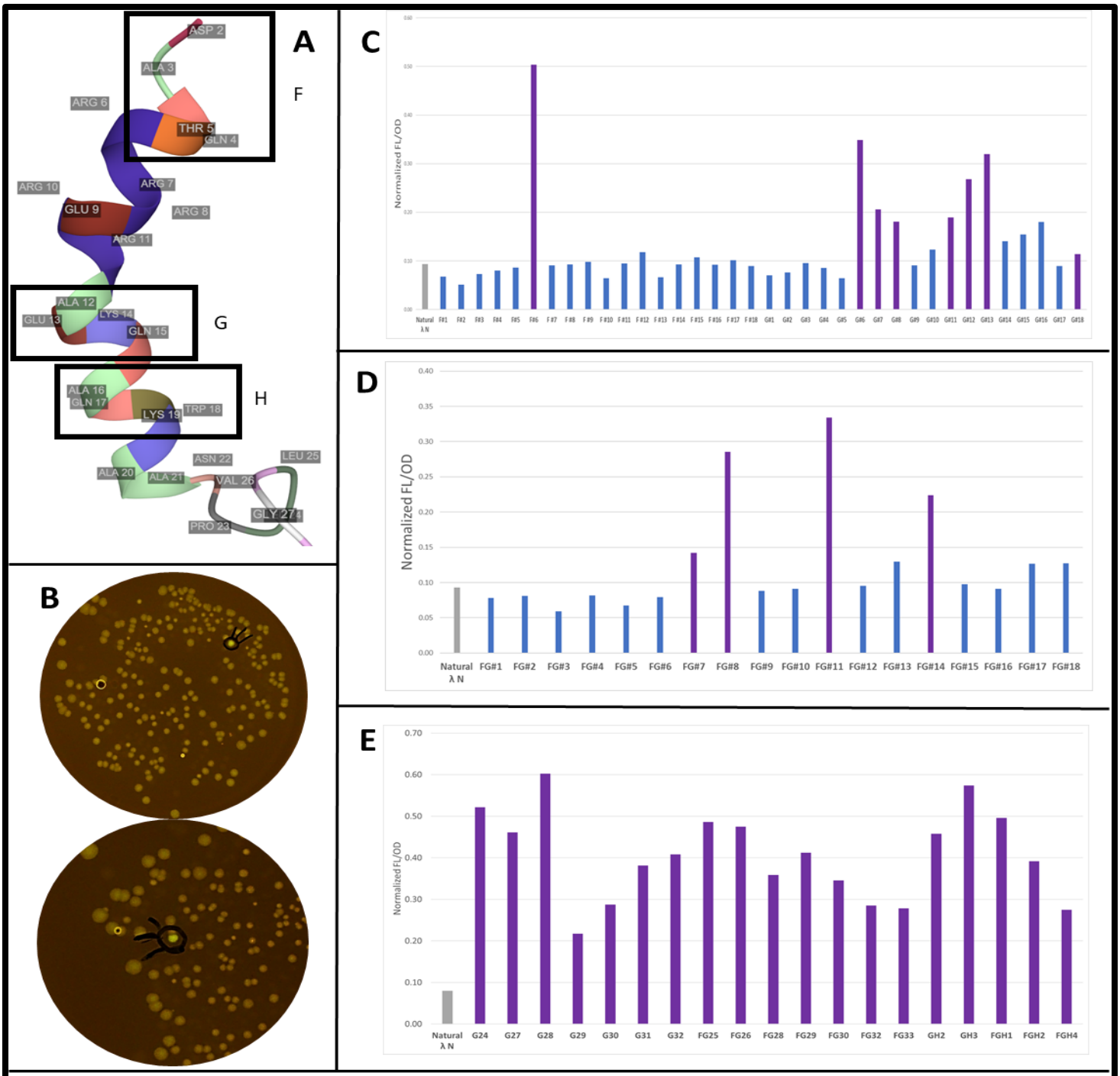

Figure 9. **Screening of randomized Escherichia phage λ (Bacteriophage λ) Antitermination N protein** (A) Identification of amino acids on NMR model of λ N protein. Amino acids in positions 2(Asp), 3(Ala), 4(Gln) and 5(Thr) were randomized together and called region F. Amino acids in positions 12 (Ala), 13(Glu), 14(Lys), and 15(Gln) were randomized together and called region G. (B) Representative plates from λ N protein randomization. All images represents the plate viewed on the dark reader. (C) Fluorescence measurements of selected single region randomized colonies compared to the natural λ N protein. (D) Fluorescence measurements of selected double region randomized (both regions F and G were randomized together) colonies compared to the natural λ N protein . (E) Fluorescence measurements of selected single, double and triple region randomized (regions F, G, H were randomized together) colonies compared to the natural λ N protein . In (C) , (D) and (E) each bar represents one colony selected from the visual screening of the colonies. Each bar is normalized to the OmpF ON control.

After observing promising results from initial rounds of randomizing the G and F regions, further rounds of randomization were performed and a third region (region H) was added for the randomization which included the amino acids in position 16 (Ala), 17 (Gln), 18 (Trp), 19 (Lys). Addition of the third region made it possible to explore many different rounds of single and collective region randomization between G, F and H regions (Figure 9). Overall, 24 candidate peptides demonstrated an increase in GFP fluorescence over the natural peptide. Sequences of all the selected peptides are shown in Table 1.

***Table 1*. Comparing amino acid sequences of the peptides generated from randomization of the λ phage N protein.** Natural λ phage N protein is highlighted in green. Shaded amino acids represent the amino acids changed from the original peptide.

	1	2	3	4	5	6	7	8	9	10	11	12	13	14	15	16	17	18	19	20	21	22
λ N	M	D	A	Q	T	R	R	R	E	R	R	A	E	K	Q	A	Q	W	K	A	A	N
F6	M	D	A	Q	T	R	R	R	E	R	R	F	N	Y	F	A	Q	W	K	A	A	N
G6	M	I	A	L	C	R	R	R	E	R	R	A	E	K	Q	A	Q	W	K	A	A	N
G7	M	L	Stop	E	A	R	R	R	E	R	R	A	E	K	Q	A	Q	W	K	A	A	N
G8	M	T	A	I	N	R	R	R	E	R	R	A	E	K	Q	A	Q	W	K	A	A	N
G11	M	V	A	I	N	R	R	R	E	R	R	A	E	K	Q	A	Q	W	K	A	A	N
G12	M	I	D	P	K	R	R	R	E	R	R	A	E	K	Q	A	Q	W	K	A	A	N
G13	M	M	A	V	K	R	R	R	E	R	R	A	E	K	Q	A	Q	W	K	A	A	N
G16	M	T	R	T	I	R	R	R	E	R	E	P	K	S	K	H	N	G	K	L	Q	
G24	M	I	A	A	I	R	R	R	E	R	R	A	E	K	Q	A	Q	W	K	A	A	N
G27	M	I	A	Y	P	R	R	R	E	R		A	E	K	Q	A	Q	W	K	A	A	N
G28	M	I	A	K	H	R	R	R	E	R	R	A	E	K	Q	A	Q	W	K	A	A	N
G29	M	I	A	K	H	R	R	R	E	R	R	A	E	K	Q	A	Q	W	K	A	A	N
G30	M	I	V	I	K	R	R	R	E	R	R	A	E	K	Q	A	Q	W	K	A	A	N
G31	M	I	A	K	Y	R	R	R	E	R	R	A	E	K	Q	A	Q	W	K	A	A	N
G32	M	I	A	R	M	R	R	R	E	R	R	A	E	K	Q	A	Q	W	K	A	A	N
FG7	M	L	S	C	S	R	R	R	E	R	R	C	F	I		A	Q	W	K	A	A	N
FG8	M	I	A	S	P	R	R	R	E	R	I	S	F	Stop		A	Q	W	K	A	A	N
FG11	M	I	A	S	P	R	R	R	E	R	I	S	F	Stop		A	Q	W	K	A	A	N
FG14	M	I	I	S	L	R	R	R	E	R	R	S	F	W	I	A	Q	W	K	A	A	N
GH2	M	A	L	N	D	R	R	R	E	R	R	A	E	K	Q	L	K	V	G	A	A	N
GH3	M	I	A	N	P	R	R	R	E	R	R	A	E	K	Q	C	M	S	G	A	A	N
FGH1	M	I	A	K	T	R	R	R	E	R	R	F	I	F	F	A	Q	W	K	A	A	N
FGH2	M	L	S	K	S	R	R	R	E	R	R	C	F	I		A	Q	W	K	A	A	N
FGH3	M	T	H	I	P	R	R	R	E													

Due to the nature of the screening method, only single colonies were generated and tested. To confirm the binding between the generated peptides and MicF, each peptide sequence was assembled into a ColE1 plasmid vector using Gibson assembly. Constructing each peptide on a separate plasmid created the opportunity to test them against proper controls. All of the

candidates were tested alongside the previously described controls: OmpF ON, ompF OFF, and AntiMicF ctrl. An additional peptide control was added to assure there is no effects from the peptide on the production of the GFP when the MicF in not present. This control only included the peptide, together with ompF-GFP and p15A control plasmid inside the cells. All conditions were tested with three biological replicates normalized to the OmpF ON control to determine the best candidate to pursue.

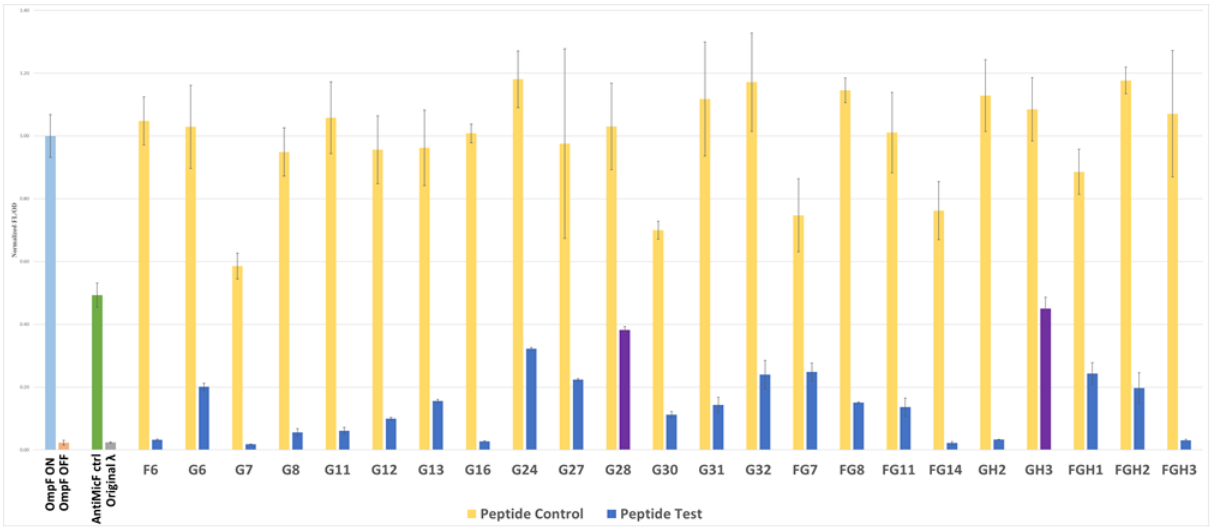

Figure 10. **Confirmation of generated peptides in triplicates with proper controls.** All measurements are normalized to the OmpF ON control. Yellow bars represent the peptide control with no MicF in the combination. Dark blue and purple bars represent the normalized FL/OD measured from the colony when MicF was present. The best candidates, G28 and GH3, are shown in purple. Error bars represent the standard deviation from three biological replicates.

As shown in Figure 10, G28 and GH3 peptide candidates were the most successful peptides generated from the randomization step. After the confirmation of the peptides in triplicates, G28 and GH3 were chosen for more thorough analysis. To start, GH3 was evaluated to determine if the change in the G or H region of the peptide was contributing to MicF binding. To investigate the effects of each region separately, from the original lambda peptide, only the desired region was mutated which made it possible to observe the effects of the G or H regions

independently and compare them to the GH3 peptide as a whole. In the figures moving forward, peptides were identified by the mutations in each of the three regions G, F, and H. The name appears in parentheses using the name of the peptide that was used to construct the peptide. For instance, GH3 will be named as (GH3, wt, GH3).

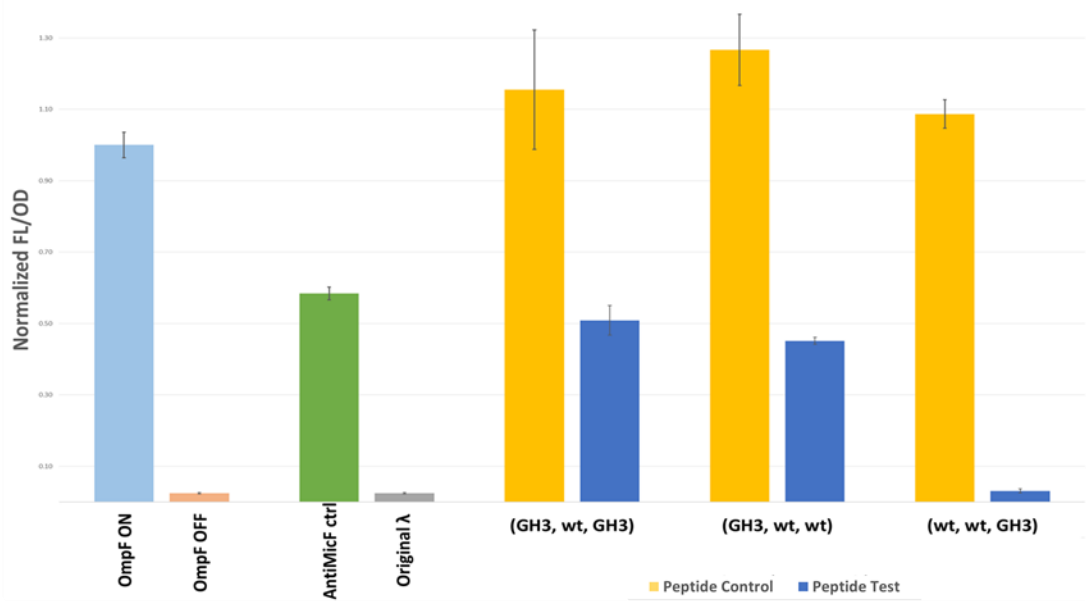

Figure11. **Determining the contribution of regions G and H from peptide GH3.** All the measurements are normalized over the OmpF ON control. Yellow bars represent the peptide control with no MicF in the combination. Dark blue bars represent the normalized FL/OD measured from the colony when MicF was present. Error bars represent the standard deviation from three biological replicates.

As seen in Figure 11, region G from GH3 (GH3, wt, wt) generated the vast amount of the fluorescence, while region H by itself (wt, wt, GH3) did not generate a substantial amount of fluorescence. However, the highest FL/OD was observed when both regions were combined together and tested as the original GH3 (GH3, wt, GH3). This observation led to an interesting question and that is: What if the region H from GH3 was added to all the other G regions generated from the randomization? Would that create a better candidate?

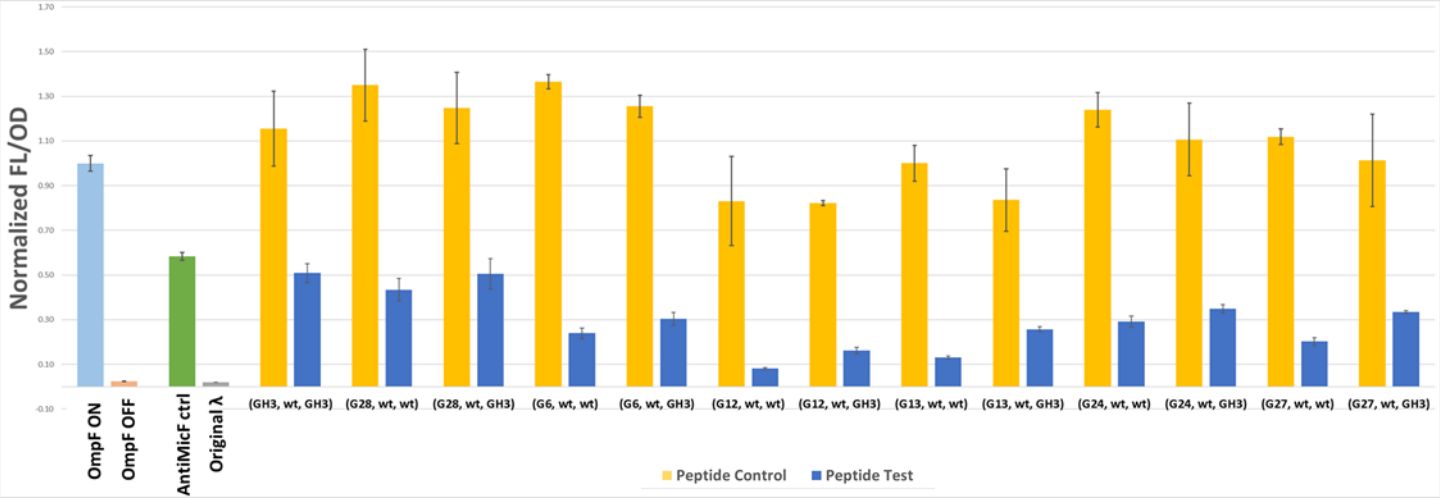

Figure 12. **Screening of peptides with an addition of H region of GH3 peptide.** All the measurements are normalized over the OmpF ON control. Yellow bars represent the peptide control with no MicF in the combination. Dark blue bars represent the normalized FL/OD measured from the colony when MicF was present. Error bars represent the standard deviation from three biological replicates.

Addition of H region from GH3 to the top performing G peptides from Figure 10 appeared to modestly increase the fluorescence compared to the original peptides with only G region randomization. However, the GH3 remained the best candidate thus far (Figure 12). This sparked an interest to randomize the F and H region one more time in order to find more capable peptides in binding to MicF. In this round of randomization, the G region was preserved from the G28 and GH3 and only F ad H regions were randomized. Figures 13 and 14 represents the randomization results for each of the conditions.

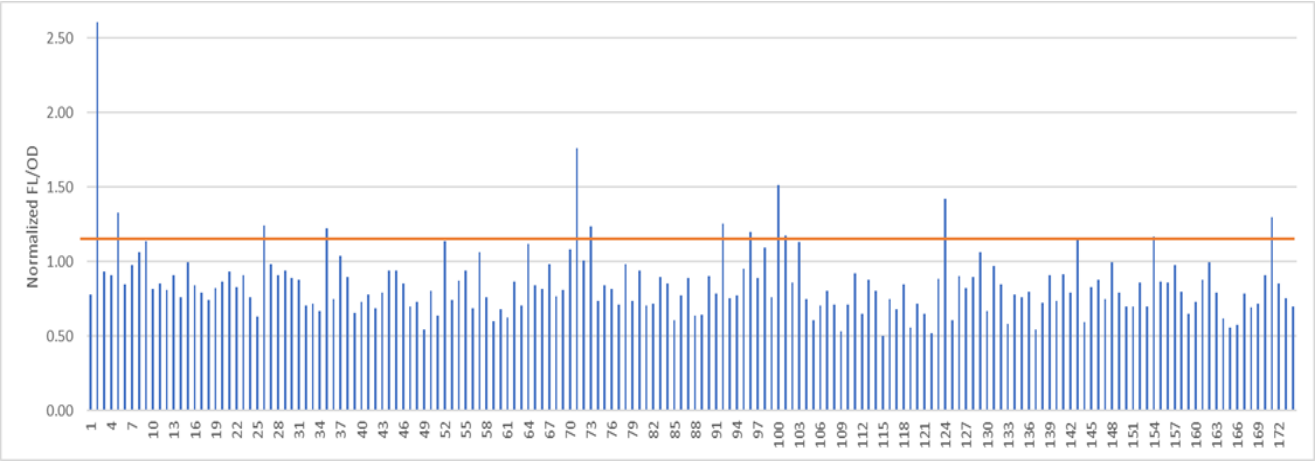

Figure 13. **Screening of colonies generated from randomizing regions F and H while preserving the G region from G28.** All the measurements are normalized over the original G28. Orange line represents the 15% increase cut off for peptide selection. Dark blue bars represent the normalized FL/OD measured from the colony.

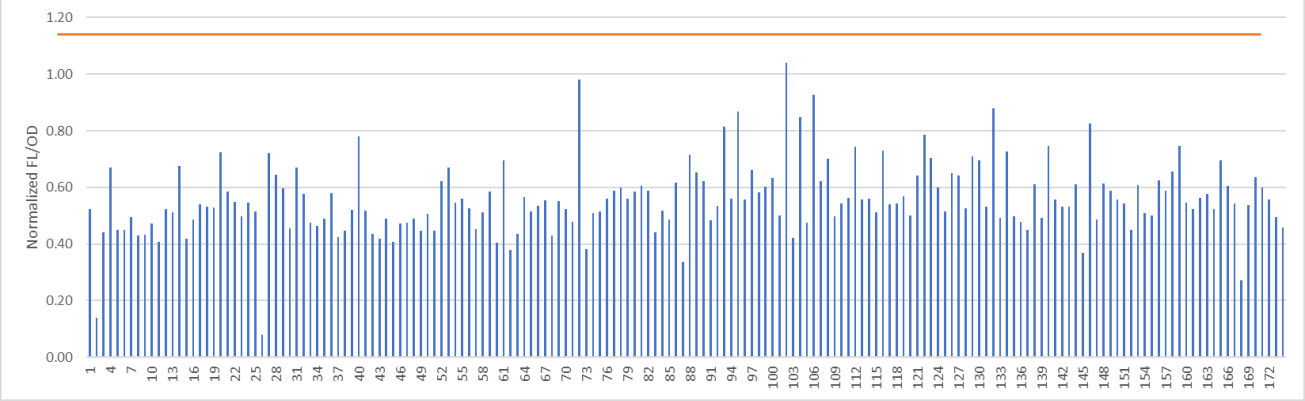

Figure 14. **Screening of colonies generated from randomizing regions F and H while preserving the G region from GH3.** All the measurements are normalized over the original GH3. Orange line represents the 15% increase cut off for peptide selection. Dark blue bars represent the normalized FL/OD measured from the colony.

After two rounds of randomization for regions F and H, 11 colonies were generated that had at least 15% increase compared to the G28 (G28, wt, wt) peptide but because no peptides with a higher fluorescence than GH3 were found, randomization for GH3 was not continued.

Successful colonies were sequenced and analyzed for specific mutations. After thorough examination of the sequences, only four candidates had adequate sequencing results. The remaining candidates showed premature termination or mixed peaks in their sequences, indicating multiple sequences. The results of sequences are shown in Table 2.

Table 2. **Comparing amino acid sequences of the green colonies generated from randomization of the G28 peptide.** Natural λ phage N protein is highlighted in green. Shaded amino acids represent the amino acids changed from the original peptide.

		G										F				H						
	1	2	3	4	5	6	7	8	9	10	11	12	13	14	15	16	17	18	19	20	21	22
λ N	M	D	A	Q	T	R	R	R	E	R	R	A	E	K	Q	A	Q	W	K	A	A	N
G28	M	I	A	K	H	R	R	R	E	R	R	A	E	K	Q	A	Q	W	K	A	A	N
G28-FH2	M	I	A	K	H	R	R	R	E	R	R	T	W	N	F	P						
G28-FH5	M	I	A	K	H	R	R	R	E	R	R	R	C	Q	L	A	V	F	I	A	A	N
G28-FH35	M	I	A	K	H	R	R	R	E	R	R	I	L	F	Y	H	I	R	D	A	A	N
G28-FH71	M	I	A	K	H	R	R	R	E	R	R	C	L	F	I	F	Y	L				

The successful candidate sequences were then cloned into the ColE1 plasmid backbone and tested in triplicate to confirm the results and effectiveness of the newly generated peptides in binding to MicF. Figure 15 shows the results generated from testing randomized peptides against ompF ON control. While the F and H regions in this round of randomizations appeared to have just a slight impact on overall peptide-MicF binding, additional rounds of randomization on these regions might generate a better candidate with higher binding affinity toward MicF. Unfortunately, when compared to G28 or GH3, the generated candidates in this round of randomizations were not noticeably superior candidates. For instance, three of the discovered candidates seemed to have an effect on the ompF-GFP to begin with since the peptide control did not recover the signal to 100% when no MicF was present. And although the (G28, FH71, FH71) recovered the signal as much as the G28, it had a premature termination and a shorter sequence. (G28, FH71, FH71) was omitted at this time for further exploration due to the capacity to

perform additional MICs; nonetheless, due to the shorter length of the peptide, this candidate may present an attractive horizon for future investigations. Since the results were so close, G28 and GH3 were chosen as the final peptides and included in the minimal inhibitory concentration analysis.

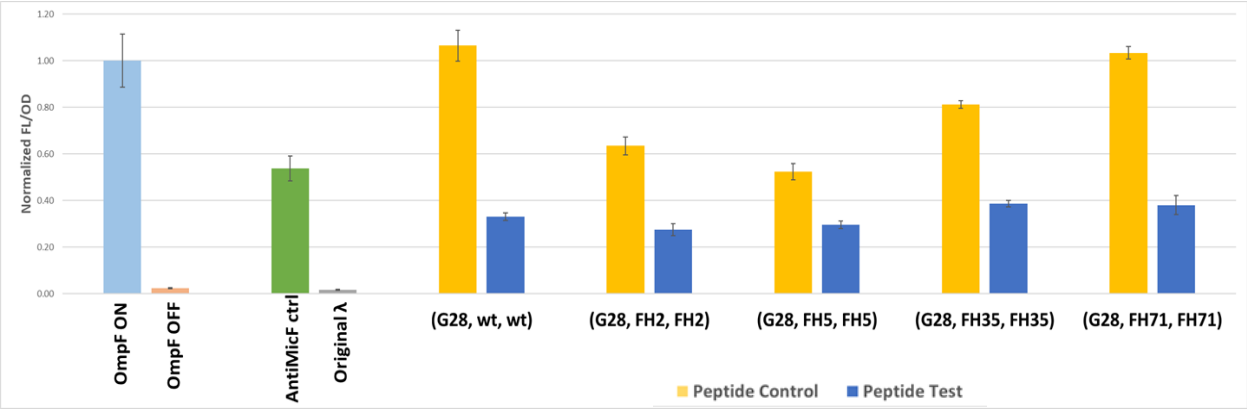

Figure 15. **Screening of the peptides from randomization of the F+H regions of G28 in triplicates** All the measurements were normalized over the OmpF ON control. Yellow bars represent the peptide control with no MicF in the combination. Dark blue bars represent the normalized FL/OD measured from the colony when MicF was present. Error bars represent the standard deviation from three biological replicates.

Minimum inhibitory concentration analysis (MIC)

This study's goal is to find the most specific and effective peptide that binds to MicF and prevents MicF from attaching to *ompF* mRNA. The genuine value of discovering such a peptide is that it can be used to increase the cell's susceptibility to antibiotics. The efficiency of GH3 and G28 peptides against two antibiotics, cephalothin and norfloxacin, was determined using MIC analysis. Cephalothin is a bactericidal antibiotic that is semisynthetic, beta-lactam, and first-generation cephalosporin. Norfloxacin is a fluoroquinolone antibiotic that belongs to the class of antibiotics known as fluoroquinolones. According to current research, when bacteria are treated with antibiotics from the beta-lactam or fluoroquinolone families, downregulation of *ompF* is a

critical line of defense [28][57]. G28 and GH3 peptide structures were constructed on ColE1 backbone using the P_{lux} inducible promoter for activation of peptides in transformed MG1655 cells. Because the peptides are on an inducible promoter, they can be expressed in the cell only when the appropriate antibiotic is present. To account for any burden on the cells due to the presence of a plasmid, MIC results were compared to cells transformed with a plasmid containing the P_{Lux} promoter without a peptide. The results of the MIC analysis showed that the MIC decreased in the presence of both peptides (Figure 16 and 17).

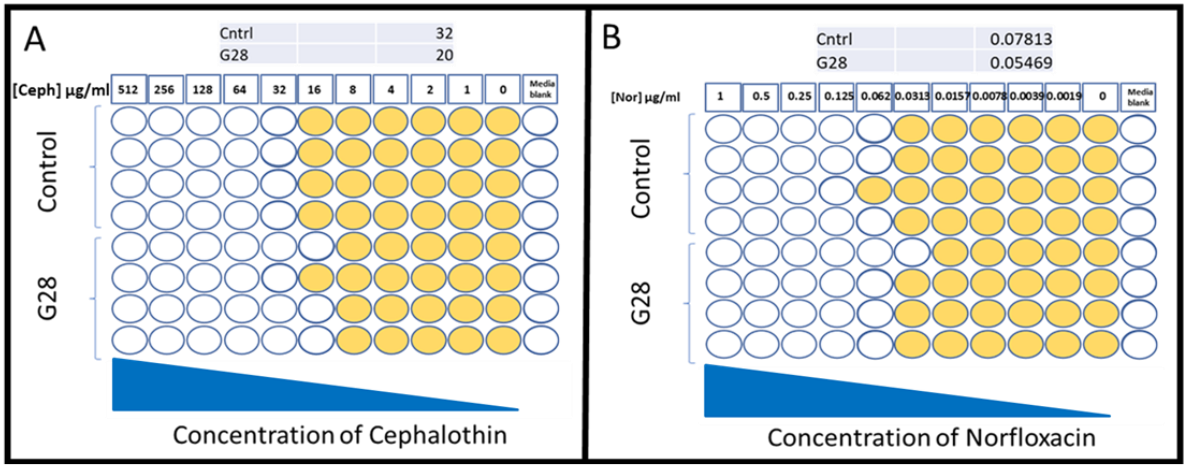

Figure 16. **Minimum inhibitory concentration analysis of the G28 peptide.** (A) MIC visualization of growth on plates per dilutions of cephalothin. (B) MIC visualization of growth on plates per dilutions of norfloxacin. Yellow circles represent the growth in the well. White circles represent no growth in the well. Rows are representation of technical replicates in experiments.

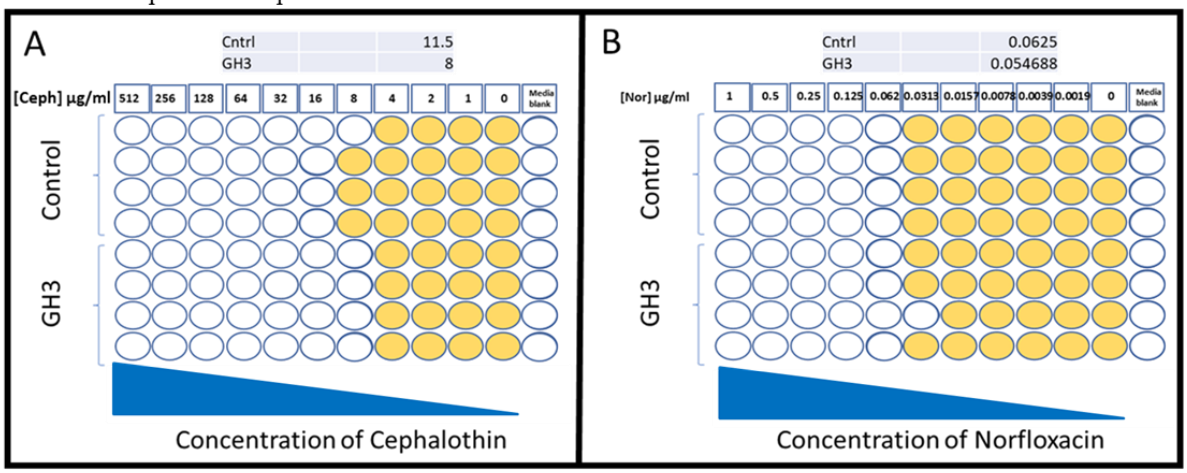

Figure 17. **Minimum inhibitory concentration analysis of the GH3 peptide.** (A) MIC visualization of growth on plates per dilutions of cephalothin. (B) MIC visualization of growth on plates per dilutions of norfloxacin. Yellow circles represent the growth in the well. White circles represent no growth in the well. Rows are representation of technical replicates in experiments.

CHAPTER 4: DISCUSSION

The loss or downregulation of porins results in reduced permeability of the outer membrane. When *E. coli* encounters antibiotics, it modulates the expression of OmpF via the upregulation of the MicF sRNA, which inhibits OmpF translation. This study paves the way for the development of a peptide capable of binding to MicF and sequester it from reaching to *ompF*. As a result, when resistance is acquired by this mechanism, the use of peptides that can bind to MicF and increase outer membrane permeability would facilitate the penetration of the antibiotic into the bacterial cell and increase susceptibility. These peptides do not need to exert antimicrobial activity but rather potentiate the effects of clinically relevant antibiotics by increasing outer membrane permeability. This makes them potentially useful for the treatment of infections caused by multi-resistant organisms due to increased permeability and may also allow, in some cases, the utilization of lower antibiotic doses. Because these peptides are particularly targeted at a sRNA that plays a role in antibiotic resistance rather than exerting antimicrobial properties on their own, no resistance from bacteria is expected to be developed anytime soon. Due to MicF's critical involvement in osmoregulation in *E. coli* cells, targeting MicF to overcome antibiotic resistance may have mild effects on cell survival. MicF is a post-transcriptional regulator in *E. coli*, and its sequestration from its ultimate target, *ompF* mRNA, would challenge the cell survival once the cell is exposed to higher osmolarity conditions. However, since the goal of the study is to stop the cell's growth and eventually kill the bacterial infections, this is not a problem.

The first goal of this study laid the way for the subsequent goals by allowing for the simultaneous screening of thousands of peptides. Bacterial fluorescent colony selection was

established as a rapid screening method to identify specific peptides available from a library containing thousands of peptide molecules using a fluorescent reporter. This was achieved by fusion of the 5' UTR region of the *ompF* to the green fluorescent protein (GFP) as a reporter to monitor the effective prevention of the MicF binding due to candidates from a library of peptides. This established method showed that detection of a specific peptide with a random mutation is possible using fluorescent selection. The system was developed on the basis of fluorescence expression and was optimized on the basis of optimal growth of the transformed cells. Initially, four natural peptides were tested. Although the results indicated no binding between MicF and the four peptides, the platform proved to be an optimal method for screening peptide candidates as seen in Aim 2.

Aim 2 of the study began by randomizing identified regions of four candidate peptides to develop an efficient peptide capable of binding to MicF. When the indicated regions were randomized, λ phage was the only contender that produced green colonies out of the four (Figure 9). Overall, three areas on the λ phage were randomized, and these three regions were used to test many combinations. The randomization of three regions yielded a total of 24 candidate peptides (Table 1). After examining the structural modifications in each sequence, it was discovered that substituting negative amino acid in position two (aspartic acid) with neutral alternatives, specifically isoleucine had a significant impact on binding ability. This observation was consistent between fourteen of the candidates that had isoleucine substitutions. Moreover, in position two of all 24 candidate peptides, the carboxyl group was substituted with a saturated hydrocarbon functional group. The peptide's methyl group (CH_3) most likely permitted it to form a hydrogen bond with MicF. Furthermore, the amino acids 4 and 5 were changed to positively charged amino acids for the majority of the peptide candidates. These changes may explain why

the peptide was allowed to interact with MicF in the first place. To further investigate the reasons that led to binding between the candidate peptides and the MicF, structural analysis was conducted using 3D visualization of the peptides. Any changes to the amino acid profile of the peptide that would lead to changes in the shape of the peptide could have an effect on binding the peptide and the MicF. The results of the 3D visualization revealed that there are no changes in the structure of the peptides when the length of the peptide is preserved. (Figure 18).

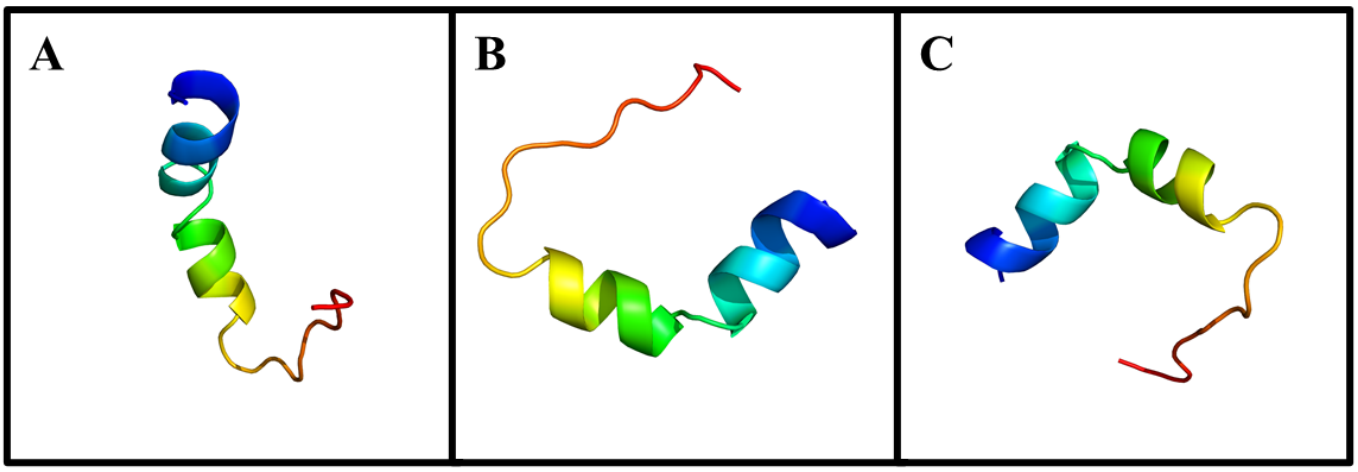

Figure 18. **3D visual analysis of G28 and GH3 compared to natural Lambda peptide** (A) 3D visualization of natural N-protein from bacteriophage λ. (B) 3D visualization of developed GH3 peptide. (B) 3D visualization of developed G28 peptide. Rainbow colors are representative of the amino acids developed by the PHYRE2 Protein Fold Recognition Server.

Out of 24 candidates, GH3 and G28, were found as potential peptides after confirmation of the results in triplicates. Following the selection of probable candidates, the research of individual areas was the next stage. Mutated regions of the GH3 peptide were examined individually to determine the impact of each region on the peptide binding affinity. Once it was discovered that the G region was the main contributor to peptide binding and that the H region was only slightly increasing binding affinity (Figure 11), it was proposed that the H region generated from the GH3 be combined with the other successful G candidates from previous rounds to produce a more potent peptide and to better understand the effects of the H region. GH3 is currently the top candidate identified in these studies, but the subsequent processes

revealed that many additional rounds of randomization could potentially yield better candidates with higher binding affinity to the RNA targets. To date, GH3 compares to antimicF 1-33, which has a high specificity and affinity for MicF, by over 80%. More rounds of randomization, as well as additional randomization regions, may yield a peptide that is as good as antimicF 1-33.

The goal of Aim 3 was to test the ability of the final candidate peptides to improve antibiotic efficacy. Recovering fluorescence signal in an experimental setup is irrelevant if the peptide is not capable of improving the effectiveness of the current antibiotics. The MIC analysis was used to get the answer to these queries. When the results of the control and candidate peptides are compared, the *E. coli* MG1655 bacteria are shown to be 30 percent more susceptible to antibiotics tested on average. The antibiotics used in this project's MIC analysis were from the beta-lactam and fluoroquinolone families. MicF-mediated downregulation of OmpF appears to have a significant effect on these two antibiotic families.

The results for norfloxacin and cephalothin were promising and demonstrated the effectiveness of the peptide candidates. Therefore, MIC testing for a wide range of antibiotics will be pursued in the future. To perform the MIC analysis, peptide candidates were expressed in the cells. These peptides must, however, be able to cross the cell membrane on their own in order to be useful. Peptides should be chemically produced and their membrane penetrating properties studied to see if they are capable of getting into cells on their own. There are two methods to study the permeability of the peptides. In the first technique, fluorescence microscopy can be used to explore the penetration properties of the candidate peptides through the *E. coli* membrane. The green fluorescent dye FITC, which is unable to pass through the cytoplasmic membrane of cells unless it has been permeabilized by the candidate peptides, can be used to complete this approach [58]. The second technique would be based on the same principles as the

bacterial fluorescent colony section that was developed for this research. In this system, two genes of interest, MicF and ompF-GFP would be minimally expressed inside the cells and chemically synthesized peptides would be introduced to the medium. The colonies will turn green if the peptide crosses the membrane and performs its purpose of binding to MicF; otherwise, the cells will remain white. If the peptides were not capable of penetrating *E. coli* on their own, they could be conjugated to known cell-penetrating peptides (CPP) such as a minimal sequence of Penetratin (RRMKWKK), that has been proven to facilitate the translocation across the cell membrane and eased the delivery of peptides allowing them to carry out their biological function [59]. Alternatively, if the cell penetration was not possible using the Penetratin, filamentous bacteriophage and phage-mimetic nanoparticles could be another candidate for delivery of the candidate peptides due to high gene loading capacity and flexible genetic engineering properties[60]. The development of resistance to peptides is another intriguing topic that should be researched further. FlAsH-based live-cell fluorescent imaging of synthetic peptides expressed inside *E. coli* can be used to examine whether cells become resistant to peptides[61]. The existence of the peptide should be evaluated after growing many generations of *E. coli*. Because of the nature of these peptides and their lack of antibacterial capabilities, no immediate resistance is envisaged; nonetheless, elimination of the peptides via efflux pumps is an option.

In conclusion, in vivo peptide selection using bacterial fluorescent colony selection enables the discovery and evolution of new peptide molecules from combinatorial libraries. These selected molecules can serve as tools to control and understand biological processes and potentially treat disease in therapeutic applications. Overall, the study of the sRNA regulation involved in antibiotic resistance through changes in porins will provide a better picture of the

processes that bacterial pathogens undergo inside the patient. At a time when the development of new antimicrobial agents based on direct bacterial inhibition is quite limited, this research endeavor should ultimately provide new adjunctive alternatives to improve the efficacy of antibiotic therapy programs. This study is directly targeting MicF production inside *E. coli*; however, MicF is highly conserved among γ-proteobacteria. In the future, this method can be applied to additional sRNAs, and design rules for peptide-RNA interactions can be developed.

LITERATURE CITED

[1] S. W. Kim *et al.*, "The importance of porins and β-lactamase in outer membrane vesicles on the hydrolysis of β-lactam antibiotics," *Int. J. Mol. Sci.*, vol. 21, no. 8, 2020.

[2] J. Davies, "Origins and evolution of antibiotic resistance.," *Microbiologia*, vol. 12, no. 1, pp. 9–16, 1996.

[3] U. Centers for Disease Control, "Antibiotic Resistance Threats in the United States, 2019."

[4] N. Mobarki, B. Almerabi, and A. Hattan, "Antibiotic Resistance Crisis," *Int. J. Med. Dev. Ctries.*, vol. 40, no. 4, pp. 561–564, 2019.

[5] L. Price and C. Liu, "What Is Antibiotic Resistance?," *Antibiot. Resist. action Cent.*, 2020.

[6] K. K. Holmes, S. Bertozzi, B. R. Bloom, P. Jha, H. Gelband, and L. M. Demaria, *Disease Control Priorities, Third Edition (Volume 6): Major Infectious Diseases*, no. Dc. 2017.

[7] B. W. Skinner, K. A. Curtis, and A. L. Goodhart, *Hypnotics and Sedatives*, vol. 40. 2018.

[8] S. Y. Tan and Y. Tatsumura, "Alexander Fleming (1881–1955): Discoverer of penicillin," *Singapore Med. J.*, vol. 56, no. 7, pp. 366–367, 2015.

[9] P. G. Pappas *et al.*, "Clinical Practice Guidelines for the Management of Candidiasis : 2009 Update by the Infectious Diseases Society of America Linked references are available on JSTOR for this article : Clinical Practice Guidelines for the Management of Candidiasis : 2009 Up," no. May, 2019.

[10] B. Li and T. J. Webster, "Bacteria antibiotic resistance: New challenges and opportunities for implant-associated orthopedic infections," *J. Orthop. Res.*, vol. 36, no. 1, pp. 22–32, 2018.

[11] M. N. Gwynn, A. Portnoy, S. F. Rittenhouse, and D. J. Payne, "Challenges of antibacterial discovery revisited," *Ann. N. Y. Acad. Sci.*, vol. 1213, no. 1, pp. 5–19, 2010.

[12] G. B. Rogers, M. P. Carroll, and K. D. Bruce, "Enhancing the utility of existing antibiotics by targeting bacterial behaviour?," *Br. J. Pharmacol.*, vol. 165, no. 4, pp. 845–857, 2012.

[13] M. Cheesman, A. Ilanko, B. Blonk, and I. E. Cock, "Pharmacognosy Reviews," vol. 1, no. 2, pp. 8–15, 2018.

[14] J. M. Munita, C. A. Arias, A. R. Unit, and A. De Santiago, "Mechanisms of Antibiotic Resistance," *HHS Public Access*, vol. 4, no. 2, pp. 1–37, 2016.

[15] S. Džidić, J. Šušković, and B. Kos, "Antibiotic resistance mechanisms in bacteria: Biochemical and genetic aspects," *Food Technol. Biotechnol.*, vol. 46, no. 1, pp. 11–21, 2008.

[16] J. M. Pagès, C. E. James, and M. Winterhalter, "The porin and the permeating antibiotic: A selective diffusion barrier in Gram-negative bacteria," *Nat. Rev. Microbiol.*, vol. 6, no.

12, pp. 893–903, 2008.

[17] H. I. Zgurskaya, C. A. Lopez, and S. Gnanakaran, “Permeability Barrier of Gram-Negative Cell Envelopes and Approaches To Bypass It,” *Physiol. Behav.*, vol. 176, no. 3, pp. 139–148, 2017.

[18] J. Vergalli *et al.*, “Porins and small-molecule translocation across the outer membrane of Gram-negative bacteria,” *Nat. Rev. Microbiol.*, vol. 18, no. 3, pp. 164–176, 2020.

[19] A. Kumar and H. P. Schweizer, “Bacterial resistance to antibiotics: Active efflux and reduced uptake,” *Adv. Drug Deliv. Rev.*, vol. 57, no. 10, pp. 1486–1513, 2005.

[20] A. H. Delcour, “Delcour, A. H. (2010). NIH Public Access, 1794(5), 808–816. http://doi.org/10.1016/j.bbapap.2008.11.005.Outer,” vol. 1794, no. 5, pp. 808–816, 2010.

[21] J. Brdin, N. Saint, M. Malle, E. De, V. Simonet, and J. Page, “Alteration of pore properties of Escherichia coli OmpF induced by mutation of key residues in anti-loop 3 region,” *Society*, vol. 528, pp. 521–528, 2002.

[22] U. Choi and C. R. Lee, “Distinct Roles of Outer Membrane Porins in Antibiotic Resistance and Membrane Integrity in Escherichia coli,” *Front. Microbiol.*, vol. 10, no. APR, pp. 1–9, 2019.

[23] D. I. Chan, E. J. Prenner, and H. J. Vogel, “Tryptophan- and arginine-rich antimicrobial peptides: structures and mechanisms of action.,” *Biochim. Biophys. Acta*, vol. 1758, no. 9, pp. 1184–1202, Sep. 2006.

[24] I. JC, O. BO, E. JO, and O. JA, “Impact of Outer Membrane Protein OmpC and OmpF on Antibiotics Resistance of *E. coli* Isolated from UTI and Diarrhoeic Patients in Zaria, Nigeria,” *Clin. Microbiol. Open Access*, vol. 05, no. 06, pp. 1–5, 2016.

[25] Nikaido H, “Outer membrane barrier as a mechanism of antimicrobial resistance,” *Antimicrob. Agents Chemother.*, vol. 33, no. 11, pp. 1831–1836, 1989.

[26] W. Achouak, T. Heulin, and J.-M. Pages, “Multiple facets of bacterial porins,” *Future Microbiol.*, vol. 6, no. 12, pp. 1415–1427, 2011.

[27] M. N. Hall and T. J. Silhavy, “The ompB locus and the regulation of the major outer membrane porin proteins of Escherichia coli K12,” *J. Mol. Biol.*, vol. 146, no. 1, pp. 23–43, 1981.

[28] M. Dupont, E. Dé, R. Chollet, J. Chevalier, and J. M. Pagès, “Enterobacter aerogenes OmpX, a cation-selective channel mar- and osmo-regulated,” *FEBS Lett.*, vol. 569, no. 1–3, pp. 27–30, 2004.

[29] N. Mizuno and S. Fujii, “Discrete-Time Adaptive Control for Continuous-Time Systems Using Limiting-Zero Model and Its Application,” *IFAC Proc. Vol.*, vol. 23, no. 1, pp. 113–118, 1990.

[30] N. Delihas and S. Forst, “MicF: An antisense RNA gene involved in response of Escherichia coli to global stress factors,” *J. Mol. Biol.*, vol. 313, no. 1, pp. 1–12, 2001.

[31] M. T. Gallegos, R. Schleif, A. Bairoch, K. Hofmann, and J. L. Ramos, “Arac/XylS family

of transcriptional regulators.," *Microbiol. Mol. Biol. Rev.*, vol. 61, no. 4, pp. 393–410, 1997.

[32] H. Hachler, S. P. Cohen, and S. B. Levy, "marA, a regulated locus which controls expression of chromosomal multiple antibiotic resistance in Escherichia coli," *J. Bacteriol.*, vol. 173, no. 17, pp. 5532–5538, 1991.

[33] T. Kim, G. Bak, J. Lee, and K. sun Kim, "Systematic analysis of the role of bacterial Hfq-interacting sRNAs in the response to antibiotics," *J. Antimicrob. Chemother.*, vol. 70, no. 6, pp. 1659–1668, 2014.

[34] M. Guillier, S. Gottesman, and G. Storz, "Modulating the outer membrane with small RNAs," *Genes Dev.*, vol. 20, no. 17, pp. 2338–2348, 2006.

[35] M. Viveiros *et al.*, "Antibiotic stress, genetic response and altered permeability of *E. coli*," *PLoS One*, vol. 2, no. 4, 2007.

[36] C. Balague and E. Garci, "Activation of Multiple Antibiotic Resistance in Uropathogenic," vol. 45, no. 6, pp. 1815–1822, 2001.

[37] J. zhong Xu, J. lan Zhang, and W. guo Zhang, "Antisense RNA: the new favorite in genetic research," *J. Zhejiang Univ. Sci. B*, vol. 19, no. 10, pp. 739–749, 2018.

[38] "Delivering the promise of RNA therapeutics," *Nat. Med.*, vol. 25, no. 9, p. 1321, 2019.

[39] J. Habault and J. L. Poyet, "Recent advances in cell penetrating peptide-based anticancer therapies," *Molecules*, vol. 24, no. 5, pp. 1–17, 2019.

[40] M. W. Hentze, A. Castello, T. Schwarzl, and T. Preiss, "A brave new world of RNA-binding proteins," *Nat. Rev. Mol. Cell Biol.*, vol. 19, no. 5, pp. 327–341, 2018.

[41] P. Thandapani, T. R. O'Connor, T. L. Bailey, and S. Richard, "Defining the RGG/RG Motif," *Mol. Cell*, vol. 50, no. 5, pp. 613–623, 2013.

[42] A. D. Frankel, "Fitting peptides into the RNA world," *Curr. Opin. Struct. Biol.*, vol. 10, no. 3, pp. 332–340, 2000.

[43] I. A. Laird-Offringa and J. G. Belasco, "Analysis of RNA-binding proteins by in vitro genetic selection: Identification of an amino acid residue important for locking U1A onto its RNA target," *Proc. Natl. Acad. Sci. U. S. A.*, vol. 92, no. 25, pp. 11859–11863, 1995.

[44] A. D. Frankel and J. A. T. Young, "HIV-1: Fifteen proteins and an RNA," *Annu. Rev. Biochem.*, vol. 67, pp. 1–25, 1998.

[45] H. P. BOGERD, H. L. WIEGAND, P. D. BIENIASZ, and B. R. CULLEN, "Functional Differences between Human and Bovine Immunodeficiency Virus Tat Transcription Factors," *J. Virol.*, vol. 74, no. 10, pp. 4666–4671, 2000.

[46] M. A. Weiss and N. Narayana, "RNA recognition by arginine-rich peptide motifs," *Biopolymers*, vol. 48, no. 2–3, pp. 167–180, 1998.

[47] K. Harada, S. S. Martin, and A. D. Frankel, "Selection of RNA-binding peptides in vivo," *Nature*, vol. 380, no. 6570. pp. 175–179, 1996.

[48] J. Tao and A. D. Frankel, “Specific binding of arginine to TAR RNA,” *Proc. Natl. Acad. Sci. U. S. A.*, vol. 89, no. 7, pp. 2723–2726, 1992.

[49] T. S. Bayer, L. N. Booth, S. M. Knudsen, and A. D. Ellington, “Arginine-rich motifs present multiple interfaces for specific binding by RNA,” *Rna*, vol. 11, no. 12, pp. 1848–1857, 2005.

[50] D. Schumacher, A. Harms, S. Bergeler, E. Frey, and L. Søgaard-4 Andersen, “PomX, a ParA/MinD ATPase activating protein, is a triple regulator of cell division in 2 Myxococcus xanthus 3,” *bioRxiv*, p. 2020.12.14.422651, 2020.

[51] F. R. Blattner *et al.*, “The complete genome sequence of Escherichia coli K-12,” *Science (80-.).*, vol. 277, no. 5331, pp. 1453–1462, 1997.

[52] Q. Yan and S. S. Fong, “Study of in vitro transcriptional binding effects and noise using constitutive promoters combined with UP element sequences in Escherichia coli,” *J. Biol. Eng.*, vol. 11, no. 1, pp. 1–11, 2017.

[53] L. Chen and A. D. Frankel, “An RNA-Binding Peptide from Bovine Immunodeficiency Virus Tat Protein Recognizes an Unusual RNA Structure,” *Biochemistry*, vol. 33, no. 9, pp. 2708–2715, 1994.

[54] A. I. Cocozaki, I. R. Ghattas, and C. A. Smith, “The RNA-binding domain of bacteriophage P22 N protein is highly mutable, and a single mutation relaxes specificity toward λ,” *J. Bacteriol.*, vol. 190, no. 23, pp. 7699–7708, 2008.

[55] F. Casu, B. M. Duggan, and M. Hennig, “The arginine-rich RNA-binding motif of HIV-1 Rev Is intrinsically disordered and folds upon RRE binding,” *Biophys. J.*, vol. 105, no. 4, pp. 1004–1017, 2013.

[56] S. R. Casjens and R. W. Hendrix, “Bacteriophage lambda: Early pioneer and still relevant,” *Virology*, vol. 479–480, pp. 310–330, 2015.

[57] M. Masi and J.-M. Pagès, “Structure, Function and Regulation of Outer Membrane Proteins Involved in Drug Transport in Enterobactericeae: the OmpF/C – TolC Case,” *Open Microbiol. J.*, vol. 7, no. 1, pp. 22–33, 2013.

[58] B. Vishnepolsky *et al.*, “De novo design and in vitro testing of antimicrobial peptides against gram-negative bacteria,” *Pharmaceuticals*, vol. 12, no. 2, 2019.

[59] K. Kanekura *et al.*, “Characterization of membrane penetration and cytotoxicity of C9orf72-encoding arginine-rich dipeptides,” *Sci. Rep.*, vol. 8, no. 1, pp. 1–11, 2018.

[60] Z. Ju and W. Sun, “Drug delivery vectors based on filamentous bacteriophages and phage-mimetic nanoparticles,” *Drug Deliv.*, vol. 24, no. 1, pp. 1898–1908, 2017.

[61] J. M. Estévez and C. Somerville, “FlAsH-based live-cell fluorescent imaging of synthetic peptides expressed in Arabidopsis and tobacco,” *Biotechniques*, vol. 41, no. 5, pp. 569–574, 2006.

APPENDIX

***Table 3*.** Plasmids used in this study.

MKT #	Description	Resistance marker	Plasmid Origin
172	J23118_ompF-GFP	Cm	SC101
173	J23118_MicF	Amp	p15A
174	J23118_antiMicF	Kan	colE1
109	J23119_antiMicF	Kan	colE1
221	J23118_control_DNA	Cm	SC101
176	J23118_control_DNA	Amp	p15A
178	J23118_control_DNA	Kan	colE1
220	P_{lux}_control	Kan	ColE1
179	J23118_P22_Nprotein	Kan	colE1
180	J23118_BIV_Tat	Kan	colE1
182	J23118_HIV_REV	Kan	colE1
184	J23118_Lambda_Nprotein	Kan	colE1

Table 4. Important DNA sequences

Description	Sequence
J23118-ompF-GFP-T1(term)	TTGACGGCTAGCTCAGTCCTAGGTATTGTGCTAGCAGACACATAAAGACACCAAACTCTCATCAATAGTTCCGTA AATTTTTATTGACAGAACTTATTGACGGCAGTGGCAGGTGTCATAAAAAAAACCATGAGGGTAATAAATAATGA TGAAGCGCAATATTCTGGCAGTGATCGTCCCTGCTAGCAAAGGAGAAGAACTTTTCACTGGAGTTGTCCCAATTC TTGTTGAATTAGATGGTGATGTTAATGGGCACAAATTTTCTGTCCGTGGAGAGGGTGAAGGTGATGCTACAAACG GAAAACTCACCCTTAAATTTATTTGCACTACTGGAAAACTACCTGTTCCGTGGCCAACACTTGTCACTACTCTGA CCTATGGTGTTCAATGCTTTTCCCGTTATCCGGATCACATGAAACGGCATGACTTTTTCAAGAGTGCCATGCCCG AAGGTTATGTACAGGAACGCACTATATCTTTCAAAGATGACGGGACCTACAAGACGCGTGCTGAAGTCAAGTTT GAAGGTGATACCCTTGTTAATCGTATCGAGTTAAAGGGTATTGATTTTAAAGAAGATGGAAACATTCTTGGACAC AAACTCGAGTACAACTTTAACTCACACAATGTATACATCACGGCAGACAAACAAAAGAATGGAATCAAAGCTAA CTTCAAAATTCGCCACAACGTTGAAGATGGTTCCGTTCAACTAGCAGACCATTATCAACAAAATACTCCAATTGG CGATGGCCCTGTCCTTTTACCAGACAACCATTACCTGTCGACACAATCTGTCCTTTCGAAAGATCCCAACGAAAA GCGTGACCACATGGTCCTTCTTGAGTTTGTAACTGCTGCTGGGATTACACATGGCATGGATGAGCTCTACAAATA AGTACGCGTGCTAGAGGCATCAAATAAAACGAAAGGCTCAGTCGAAAGACTGGGCCTTTCGTTTTATCTGTTGTT TGTCGGTGAACGCTCTCCTGAGTAGGACAAAT
J23118-MicF-T1(term)	TTGACGGCTAGCTCAGTCCTAGGTATTGTGCTAGCGCTATCATCATTAACTTTATTTATTACCGTCATTCATTTCTG AATGTCTGTTTACCCCTATTTCAACCGGATGCCTCGCATTCGGTTTTTTTTGCATCAAATAAAACGAAAGGCTCAG TCGAAAGACTGGGCCTTTCGTTTTATCTGTTGTTTGTCGGTGAACGCTCTCCTGAGTAGGACAAAT
J23118-antiMicF-T1 (term)	TTGACGGCTAGCTCAGTCCTAGGTATTGTGCTAGCATGACGGTAATAAATAAAGTTAATGATGATAGCGCATCAA ATAAAACGAAAGGCTCAGTCGAAAGACTGGGCCTTTCGTTTTATCTGTTGTTTGTCGGTGAACGCTCTCCTGAGT AGGACAAAT
J23118-ctrl-T1 (term) pSC101	TTGACGGCTAGCTCAGTCCTAGGTATTGTGCTAGCGAATTCGTACGCGTGCTAGAGGCATCAAATAAAACGAAA GGCTCAGTCGAAAGACTGGGCCTTTCGTTTTATCTGTTGTTTGTCGGTGAACGCTCTCCTGAGTAGGACAAATCC GCCGCCCTAGA
J23118-ctrl-T1 (term) p15A	TTGACGGCTAGCTCAGTCCTAGGTATTGTGCTAGCGAATTCGTACGCGTGCTAGAGGCATCAAATAAAACGAAA GGCTCAGTCGAAAGACTGGGCCTTTCGTTTTATCTGTTGTTTGTCGGTGAACGCTCTCCTGAGTAGGACAAATCC GCCGCCCTAGA
J23118-ctrl-T1 (term) ColE1	TTGACGGCTAGCTCAGTCCTAGGTATTGTGCTAGCGAATTCGTACGCGTGCTAGAGGCATCAAATAAAACGAAA GGCTCAGTCGAAAGACTGGGCCTTTCGTTTTATCTGTTGTTTGTCGGTGAACGCTCTCCTGAGTAGGACAAATCC GCCGCCCTAGA

***Table 5*.** Natural ARM sequences obtained from the literature along with *E. coli* codon optimized sequences of the Natural ARMs.

Peptide	Natural peptide sequences	Codon Optimized Sequence for E.Coli
TAT BIV	AGCGGCCCGCGCCCGCGCGGCACCCGCGGCAAA GGCCGCCGCATTCGCCGC	AGCGGTCCTCGTCCGCGTGGAACAAGAGGGAA AGGTCGGAGAATTCGTCGC
HIV1 - REV	ACCCGCCAGGCGCGCCGCAACCGCCGCCGCCGC TGGCGCGAACGCCAGCGC	ACCAGACAAGCTCGGCGTAACAGAAGACGCAG ATGGCGGGAGCGTCAACGC
N protein bacteriophage p22	AACGCGAAAACCCGCCGCCATGAACGCCGCCGC AAACTGGCGATTGAACGC	AACGCCAAGACACGTCGCCATGAACGTCGTCG GAAACTTGCCATCGAACGC
N protein λ Phage	ATGGATGCGCAGACCCGCCGCCGCGAACGCCGCGC GGAAAAACAGGCGCAGTGGAAAGCGGCGAAC	ATGGACGCGCAGACACGTCGGCGCGAACGGAGAG CCGAAAAGCAAGCACAATGGAAAGCTGCAAAC

Table 6. Primers designed for iPCR and Gibson Assembly.

Primers	Forward Sequence (5'–3')	Reverse Sequence (5'–3')
SC101_Backbone Gibson Assembly	CAAATAAAACGAAAGGCTCAGTCG	GACTCCTGTTGATAGATCCAGTAATGAC
SC101_Backbone Gibson Assembly	GCGAAACGATCCTCATCCTGTC	CTCGAGGTGAAGACGAAAGG
Cm^R_insertion in the backbone	TGGATCTATCAACAGGAGTCCCAGGGGTCCCCAA TAATTACG	CAGGATGAGGATCGTTTCGCGCAGCGGAAAAGGA CAAAAGTCAA
ompF-GFP_insertion in the backbone	CCTTTCGTCTTCACCTCGAGTTGACAGCTAGCTCA GTCCTAGG	TCGACTGAGCCTTTCGTTTTATTTGATGCCTCTAGC ACGCGTAC
MicF_Backbone Gibson Assembly	GCATCAAATAAAACGAAAGGCTCAGTCG	ACTAGTATTATACCTAGGACTGAGCTAGCTGT
MicF_insertion in the backbone	ACAGCTAGCTCAGTCCTAGGTATAATACTAGT	CGACTGAGCCTTTCGTTTTATTTGATGC
BIV_Tat randomization (A)	AGAGGGAAAGGTCGGAGAATTCGTCGCTAAGTAC GCGTGCTAGAGGCAT	NNNNNNACGCGGACGAGGACCGCTCATGGTACCT TTCTCCTCTTTAATGAATTCG
BIV_Tat randomization (B)	AGANNNAAAGGTCGGAGAATTCGTCGCTAAGTAC GCGTGCTAGAGGCAT	ACGTTCATGGCGACGTGTCTTGGCGTTCATGGTAC CTTTCTCCTCTTTAATGAATTCG
BIV_Tat randomization (AB)	AGANNNAAAGGTCGGAGAATTCGTCGCTAAGTAC GCGTGCTAGAGGCAT	NNNNNNACGCGGACGAGGACCGCTCATGGTACCT TTCTCCTCTTTAATGAATTCG
P22_Nprotein (C)	CGTCGGNNNNNNNNNNNNNNCGCTAAGTACGC GTGCTAGAGGCAT	ATGGCGACGTGTCTTGGCGTTCATGGTACCTTTCT CCTCTTTAATGAATTCACT
P22_Nprotein (D)	CGTCGGAAACTTGCCATCGAACGCTAAGTACGCG TGCTAGAGGCAT	ACGTTCATGGCGACGNNNNNNNNNNNNCATGGTA CCTTTCTCCTCTTTAATGAATTCG
P22_Nprotein (CD)	CGTCGGNNNNNNNNNNNNNNCGCTAAGTACGC GTGCTAGAGGCAT	ACGTTCATGGCGACGNNNNNNNNNNNNCATGGTA CCTTTCTCCTCTTTAATGAATTCG
HIV1_REV randomization	AGAAGACGCAGATGGCGGGAGCGTCAACGCTAAG TACGCGTGCTAGAGGCAT	GTTACGCCGNNNNNNTCTNNNCATGGTACCTTTCT CCTCTTTAATGAATTCG
λ phage_N protein randomization (F)	GGAGANNNNNNNNNNNNGCACAATGGAAAGCTG CAAACTAAGTACGCGTGCTAGAGGCAT	GTTCGCGCCGACGNNNNNNNNNNNNCATCATGGT ACCTTTCTCCTCTTTAATGAATTCG
λ phage_N protein randomization (G)	GGAGAGCCGAAAAGCAAGCACAATGGAAAGCTG CAAACTAAGTACGCGTGCTAGAGGCAT	GTTCGCGCCGACGNNNNNNNNNNNNCATCATGGT ACCTTTCTCCTCTTTAATGAATTCG
λ phage_N protein randomization (H)	GGAGAGCCGAAAAGCAANNNNNNNNNNNNGCTG CAAACTAAGTACGCGTGCTAGAGGCAT	GTTCGCGCCGACGTGTCTGCGCGTCCATCATGGTA CCTTTCTCCTCTTTAATGAATTCG
λ phage_N protein randomization (FG)	GGAGANNNNNNNNNNNNGCACAATGGAAAGCTG CAAACTAAGTACGCGTGCTAGAGGCAT	GTTCGCGCCGACGNNNNNNNNNNNNCATCATGGT ACCTTTCTCCTCTTTAATGAATTCG

λ phage_N protein randomization (FGH)	GGAGANNNNNNNNNNNNNNNNNNNNNNGCTGCAAACTAAGTACGCGTGCTAGAGGCAT	GTTCGCGCCGACGNNNNNNNNNNNNCATCATGGTACCTTTCTCCTCTTTAATGAATTCG
Sequencing primers	GCGTGCAATCCATCTTGTTCAATCAT	TTACCGGGTTGGACTCAAGACGA
P_{lux} Insertion primers	GTATCACGAGGCCGAATTCGCGGCCGCTTCTAGAG	TTCTCCTCTTTAATGAATTCTTTATTCGACTATAACAAACCATTTTCTTGCGTAAACC
P_{lux} Backbone primers	TGGTTTGTTATAGTCGAATAAAGAATTCATTAAAGAGGAGAAAGGTACCATG	CGGCCGCGAATTCGGCCTCGTGATACGCCTATT